Inclusive two-gluon and valence-quark-gluon production in DIS and pA collisions

Jamal Jalilian-Marian[1] and Yuri V. Kovchegov[2]

[1]*Institute for Nuclear Theory, University of Washington, Box 351550, Seattle, Washington 98195, USA*
[2]*Department of Physics, University of Washington, Box 351560, Seattle, Washington 98195, USA*

(Received 1 June 2004; published 9 December 2004)

We calculate production cross sections of a forward quark-gluon pair and of two gluons at midrapidity in deep inelastic scattering and in high energy proton-nucleus collisions. The calculation is performed in the framework of the color glass condensate formalism. We first calculate the cross sections in the quasiclassical approximation, which includes multiple rescatterings in the target. We then proceed to include the effects of nonlinear small-x evolution in the production cross sections. It is interesting to note that our result for the two-gluon production cross section appears to be in direct violation of Abramovsky-Gribov-Kanchelli cutting rules, which is the first example of such violation in QCD. The calculated quark-gluon and gluon-gluon production cross sections can be used to construct theoretical predictions for two-particle azimuthal correlations at the Relativistic Heavy Ion Collider and LHC ($I^{p(d)A}$) as well as for deep inelastic scattering experiments at the Hadron Electron Ring Accelerator and the Electron-Relativistic Heavy Ion Collider.

DOI: 10.1103/PhysRevD.70.114017 PACS numbers: 13.60.Hb, 13.85.Hd, 13.85.Ni

I. INTRODUCTION

Recent prediction of high-p_T suppression in the nuclear modification factor R^{dA} at forward rapidity Relativistic Heavy Ion Collider (RHIC) dAu collisions [1–3] based on the physics of parton saturation/color glass condensate (CGC) [4–11] has been confirmed by the experimental data in Refs. [12–16]. The prediction of Ref. [2] was based on the calculation of inclusive gluon production cross section in deep inelastic scattering (DIS) and pA collisions. The calculation was first done in the quasiclassical framework of the McLerran-Venugopalan model including all multiple rescatterings [17] (see also [18–21]). The effects of nonlinear small-x evolution [9,10,22] were included in the obtained formula in Ref. [23] (see also [24]). In Refs. [2,3] it was argued that at lower energies/rapidities, where the particle production is given by the quasiclassical formula from Ref. [17], the nuclear modification factor R^{pA} should exhibit low-p_T suppression together with a strong enhancement at high p_T, known as the Cronin effect [25] (see also [26–29] for similar conclusions). However, at higher energies/rapidities, when quantum evolution becomes important, one should expect suppression of R^{pA} at all p_T [1–3] due to the onset of Balitsky-Fadin-Kuraev-Lipatov (BFKL) anomalous dimension for gluon distributions [30]. (It had been earlier suggested in Ref. [31] that the forward rapidity region would be most sensitive to small-x evolution effects.) Similar argument about enhancement and suppression can be carried through for the valence-quark production cross section calculated in Ref. [31]. The suppression has been confirmed experimentally in Refs. [12,13]. The centrality dependence of the observed suppression was also in agreement with the predictions of the color glass condensate formalism [2]. Further developments in the area included an analysis of running coupling corrections [32] and a study of similar suppression in dilepton production [33] (see also [34]). Recently, more quantitative analyses [35,36] based on the color glass condensate formalism have been performed which show good agreement with the data [12,13].

Another distinctive prediction of the color glass condensate [4–10] is the disappearance of back-to-back jets in the low $p_T < Q_s$ and intermediate $p_T \gtrsim Q_s$ transverse momentum regions. While the single particle spectra in dAu collisions at RHIC have been successfully described by CGC-inspired models [35,36], it is important to go beyond single particle spectra and probe other observables, such as two-particle correlations, in order to map out the region of phase space where CGC is the dominant physics. The inclusive two-particle (gluon) cross section at high energy is given by the k_T factorization [37] in the high p_T region ($p_T \gg Q_s$) with the gluon distribution function evolving via the BFKL evolution equation [30]. Models based on k_T factorization have been applied to many different processes, such as the nonflow contribution to the elliptic flow observable v_2 in heavy ion collisions [38]. Recently, a similar model of two-particle correlations in dA was used in Ref. [39] to predict broadening and disappearance of back-to-back correlations in pA (or dA) collisions. The predictions of Ref. [39] appear to be confirmed by the preliminary data reported in Ref. [40], thus strengthening the case for saturation/color glass condensate in dAu data at RHIC.

Nevertheless, a theoretically rigorous treatment of inclusive two-particle production in DIS and proton-nucleus collisions in the low p_T region ($p_T \lesssim Q_s$) has not been performed yet. It is clearly needed in order to provide reliable predictions in the $p_T \lesssim Q_s$ momentum region, which is the region where the new physics of CGC is expected to be most pronounced. (Very recently, there

has been a series of articles investigating quark-antiquark production in pA collisions using the quasiclassical approximation in the CGC formalism [41].)

Our goal in this work is to derive inclusive two-particle production cross sections using the color glass condensate formalism. We start by considering production of two gluons. We assume that the two gluons are separated by a large rapidity interval so that their respective rapidities are ordered, $y_2 \gg y_1$. This kinematics is, for instance, relevant to the case of two-particle production in $p(d)A$ collisions (for example, at RHIC or LHC) when one of the produced particles is in the midrapidity region while the second particle is closer to the forward rapidity region. In Sec. II, we derive an expression for a two-gluon inclusive cross section in DIS, using the quasiclassical approximation (the McLerran-Venugopalan model) in the color glass condensate formalism and making the large-N_c approximation to simplify the calculations. (The quasiclassical approximation employed here is identical to the one used in Refs. [17–19] to describe single gluon production.) The result for a two-gluon production cross section in the quasiclassical approximation is given by Eqs. (1) and (13). We note that a similar expression for a two-quark production cross section was obtained previously for DIS in Ref. [42]. In Sec. III, we include the effects of nonlinear small-x evolution [9] in the two-gluon inclusive cross section obtained in Sec. II. The final answer for the two-gluon inclusive cross section for DIS is given in Eq. (32). This result can be easily generalized to pA collisions.

An ansatz for a two-gluon inclusive cross section including saturation effects was written in Ref. [24] inspired by k_T factorization together with Abramovsky-Gribov-Kanchelli (AGK) cutting rules [43]. We note that the diagrammatic structure of our answer in Eq. (32) does not seem to adhere to AGK cutting rules' expectation for a two-gluon inclusive cross section. Furthermore, we are unable to cast the expression (32) into the k_T-factorized form used in Ref. [24]. However, the leading-twist k_T-factorization expression [23,37] can be reproduced exactly from Eq. (32), as will be discussed at the end of Sec. III.

In Sec. IV we calculate the inclusive production of a valence-quark and a gluon in pA collisions both in the quasiclassical approximation and including the quantum evolution in the target. The rapidities of the valence-quark and the gluon are assumed to be comparable and large (both quark and gluon are produced in the forward rapidity region). The result is given by Eqs. (76)–(78). These expressions together with Eq. (32) can be used to describe the nuclear modification factor for azimuthal correlations I^{dAu} at any rapidity between midrapidity and the deuteron beam at RHIC. In particular, Eq. (32) provides the theoretical basis for the correlation analysis carried out in Ref. [39].

II. TWO-GLUON PRODUCTION IN THE QUASICLASSICAL APPROXIMATION

In this section we are going to derive an expression for an inclusive two-gluon production cross section in DIS including all multiple rescatterings of the two produced gluons and the quark-antiquark pair on the nucleons in the target nucleus [7,8,44]. A typical diagram contributing to the process is shown in Fig. 1. The two produced gluons have transverse momenta $\underline{k}_1$ and $\underline{k}_2$ and rapidities y_1 and y_2, correspondingly. To simplify the calculations we will consider the case when $y_2 \gg y_1$. A more general case of $y_2 \sim y_1$ was considered in Ref. [45] for two-gluon production at the leading-twist level given by k_T factorization. Our goal here is to include the saturation effects in the two-gluon production cross section, which means summing all twists. We will achieve this difficult task only for a simpler case of $y_2 \gg y_1$, though, in principle, the more general case $y_2 \sim y_1$ presents no new conceptual difficulties and is only technically more complicated.

As shown in Fig. 1 the gluon production process in DIS in the quasiclassical approximation [7,8,44] consists of two factorizable stages. First, the incoming virtual photon splits into a quark-antiquark pair, which emits two gluons in the incoming wave function. (The time scale for this splitting and gluon emissions is much longer than the time of interaction with the target.) The whole system multiply rescatters on the nuclear target. (In general, the gluon emissions can happen after the interaction with the target, as will be discussed shortly.) In the quasiclassical approximation considered here, the interactions with the nucleons are limited to no more than two exchanged gluons per nucleon (see the second reference in Ref. [8]). Single gluon production in the same approximation was calculated for pA collisions in Ref. [17] and for DIS in Ref. [20].

Let us assume that the virtual photon has a large "+" component of the momentum and the nucleus has a large "−" component of its momentum. Then the diagram of the process shown in Fig. 1 is dominant in $A^+ = 0$ gauge. In this section we will perform all the calculations in the framework of the light cone perturbation theory in $A^+ = 0$ gauge [46]. First of all, let us explicitly factor out the

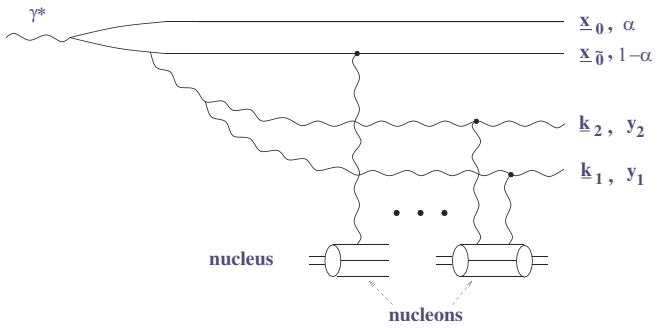

FIG. 1 (color online). Two-gluon production in DIS on a nucleus including multiple rescatterings.

wave function $\Phi^{\gamma^*\to q\bar{q}}(\underline{x}_{0\tilde{0}}, \alpha)$ of the virtual photon splitting in a quark-antiquark pair of transverse size $\underline{x}_{0\tilde{0}} = \underline{x}_0 - \underline{x}_{\tilde{0}}$ with the quark carrying a fraction α of the virtual photon's light cone momentum. The wave function $\Phi^{\gamma^*\to q\bar{q}}(\underline{x}_{0\tilde{0}}, \alpha)$ is a well-known function and can be found, for example, in Refs. [47,48]. The two-gluon inclusive production cross section can be written as

$$\frac{d\sigma^{\gamma^* A\to q\bar{q}GGX}}{d^2k_1 dy_1 d^2k_2 dy_2} = \frac{1}{2\pi^2}\int d^2x_{0\tilde{0}}\int_0^1 d\alpha \Phi^{\gamma^*\to q\bar{q}}(\underline{x}_{0\tilde{0}}, \alpha) \times \frac{d\hat{\sigma}^{q\bar{q}A\to q\bar{q}GGX}}{d^2k_1 dy_1 d^2k_2 dy_2}(\underline{x}_{0\tilde{0}}). \quad (1)$$

A. Time-ordering rules

To calculate a two-gluon production cross section for a quarkonium scattering on a nucleus, similarly to Refs. [17,20] one has to consider various possible ordering of the emissions of the two gluons by the $q\bar{q}$ pair. The interaction with the nucleus target can be considered instantaneous compared to long lifetimes of emitted gluons. Thus, we will denote the moment of interaction with the target by the light cone time $\tau \equiv x^+ = 0$. If τ_1 and τ_2 are the times of the emission of the two gluons, the possible emission ordering in the amplitude reduces to three cases: (i) both gluons are emitted before the interaction, $\tau_1, \tau_2 < 0$; (ii) one gluon is emitted before the interaction and the other one is emitted after the interaction, $\tau_1 < 0 < \tau_2$ or $\tau_2 < 0 < \tau_1$; (iii) both gluons are emitted after the interaction, $\tau_1, \tau_2 > 0$.

The three cases are represented in Fig. 2 for a particular coupling of the two gluons to the $q\bar{q}$ pair. There the dashed line in the middle denotes the (instantaneous) interaction with the target. The dashed line comprises *all* the multiple rescatterings like the ones shown in Fig. 1. The dotted lines represent intermediate states, which will give energy denominators in light cone perturbation theory [46]. Even though Fig. 2 shows a particular way of the gluons coupling to the $q\bar{q}$ pair, the conclusions we will draw below about which diagrams dominate will be applicable to other couplings of the gluons.

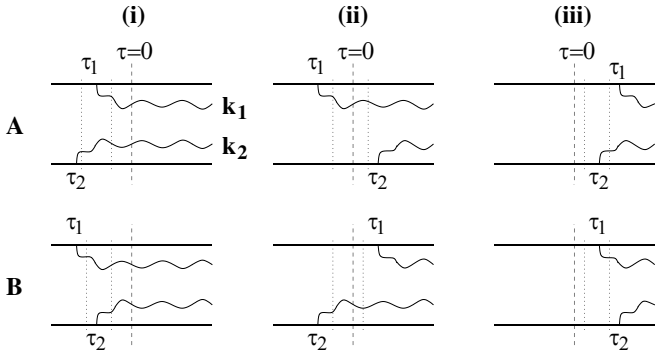

FIG. 2. Possible orderings of the emission of the two gluons by the quark-antiquark pair.

Let us define the light cone energy of a gluon or a quark line carrying momentum $(\underline{k}, k^+)$ as [46]

$$E_k \equiv k^- = \frac{\underline{k}^2}{2k^+}. \quad (2)$$

In Regge kinematics that we consider here, the light cone momenta of the gluons are ordered, such that $k_2^+ \gg k_1^+$ and $E_{k_2} \ll E_{k_1}$. First, we consider case (i) in Fig. 2. The diagrams (i)A and (i)B (top and bottom) are different only by energy denominators. Therefore, forgetting the rest of the diagram for now, we write

$$\text{(i)A} \sim \frac{1}{E_{k_2}}\frac{1}{E_{k_1}+E_{k_2}} \approx \frac{1}{E_{k_2}}\frac{1}{E_{k_1}} \quad (3)$$

and

$$\text{(i)B} \sim \frac{1}{E_{k_1}}\frac{1}{E_{k_1}+E_{k_2}} \approx \frac{1}{E_{k_1}^2}. \quad (4)$$

The intermediate states giving the energy denominators in Eqs. (3) and (4) are shown by dotted lines in Fig. 2. Since $E_{k_2} \ll E_{k_1}$, Eqs. (3) and (4) imply that (i)A $\gg$ (i)B. Therefore, diagram (i)B can be safely neglected. The conclusion we draw from this analysis is that for gluon emissions before the interaction ($\tau_1, \tau_2 < 0$) the (longitudinally) harder gluon has to be emitted first, as pictured in diagram (i)A in Fig. 2.

In calculating diagrams (i)A and (i)B, we have neglected the $-$ component of the momenta of the $q\bar{q}$ pair because they are negligibly small. The quark and the antiquark carry a very large $+$ component of the momentum, of the order of $p^+ \gg k_2^+ \gg k_1^+$, which leads to negligibly small light cone energy E_p. We have also neglected the change in the $-$ component of the target momentum, since the interaction with the target took place after the intermediate states which gave the energy denominators in case (i) in Fig. 2. This is not the case in the rest of the diagrams in Fig. 2. The $-$ momentum/light cone energy of the target changes due to the interaction (dashed line). However, since the light cone energy is conserved in the final state ($\tau = +\infty$), the change of the target's $-$ momentum is compensated by the change of the $-$ momentum of the projectile, which is mostly due to the appearance of two extra gluons leading to an addition of extra $E_{k_1} + E_{k_2}$ to the $q\bar{q}$ wave function's light cone energy. Therefore, the target's light cone energy decreases by $E_{k_1} + E_{k_2}$ after the interaction. Thus, when calculating the energy denominators of the intermediate states after the interaction, one has to add the change in the light cone energy of the target to the energies of the lines shown in Fig. 2. This is equivalent to subtracting $E_{k_1} + E_{k_2}$ in the corresponding energy denominators. (This rule is worked out in more detail in Sec. IIIA of Ref. [23].)

Guided by the rule we just derived, we write for the energy denominators of the diagrams in case (ii) in Fig 2

$$\text{(ii)A} \sim \frac{1}{E_{k_1}} \frac{1}{E_{k_1} - (E_{k_1} + E_{k_2})} = -\frac{1}{E_{k_1}} \frac{1}{E_{k_2}}, \quad (5)$$

$$\text{(ii)B} \sim \frac{1}{E_{k_2}} \frac{1}{E_{k_2} - (E_{k_1} + E_{k_2})} = -\frac{1}{E_{k_2}} \frac{1}{E_{k_1}}. \quad (6)$$

As we see from Eqs. (5) and (6), the two diagrams are of the same order, (ii)A $\sim$ (ii)B [$\sim$ (i)A], and neither of them can be neglected. [As we will see below, diagrams (ii)A and (ii)B are different in the parts responsible for the interaction with the target, so while being parametrically of the same order, they are not identically equal.]

Finally, calculating the graphs in case (iii) of Fig. 2, one arrives at

$$\text{(iii)A} \sim \frac{1}{E_{k_1} + E_{k_2}} \frac{1}{E_{k_1}} \approx \frac{1}{E_{k_1}^2} \quad (7)$$

and

$$\text{(iii)B} \sim \frac{1}{E_{k_1} + E_{k_2}} \frac{1}{E_{k_2}} \approx \frac{1}{E_{k_1}} \frac{1}{E_{k_2}}. \quad (8)$$

Since $E_{k_1} \gg E_{k_2}$ we conclude that (iii)A $\ll$ (iii)B. Diagram (iii)A should be neglected. Therefore, we derive a rule for late-time emissions, which take place after the interaction ($\tau_1, \tau_2 > 0$): the harder gluon has to be emitted *after* the softer gluon. It is interesting to note that this ordering is the exact inverse of the ordering giving the leading contribution at early times before the interaction. The rule can also be generalized to any number of gluon emissions contributing to the BFKL [30] or, equivalently, dipole evolution [9,49]: in the evolution at early times preceding the interaction, the gluons are ordered so that the harder gluons are emitted before the softer ones [49]. The ordering is reversed for late times following the interaction, where the harder gluons should be emitted after the softer gluons to pick up the leading logarithmic contribution. This observation was made previously in Ref. [23].

B. Two-gluon inclusive cross section in the quasiclassical approximation

The diagrams contributing to emission of the harder gluon with momentum ($\underline{k}_2, y_2$) are shown in Fig. 3. [In the following, we will refer to this gluon as gluon #2 and to the other (softer) produced gluon as gluon #1.] To simplify the color algebra, we will continue the calculation in 't Hooft's large-N_c limit. Only planar diagrams will contribute for gluon emission. Using the notation from Mueller's dipole model [49,50], we denote the gluon in the large-N_c limit by a double quark line and leave the ends of the gluon line disconnected from the quark lines. The latter notation indicates a sum over all possible connections of the gluon to the $q\bar{q}$ pair.

As in Fig. 2, the dashed lines in Fig. 3 denote the $\tau = 0$ moment of the interaction of the system with the target nucleus. However, unlike in Fig. 2, in Fig. 3 we depict the squares of the amplitude contributing to the total production cross section. Therefore, each diagram has two dashed lines corresponding to interaction with the target in the amplitude and in the complex conjugate amplitude. The solid vertical lines denote the final state at $\tau = +\infty$.

Similar to Mueller's dipole model [49], the emitted gluon #2 in Fig. 3(a) splits dipole $0\tilde{0}$ into two color dipoles. The emission of the softer gluon #1 can happen in either of these two dipoles. However, the original dipole model [49] was written for the calculation of the total cross sections, where one has to calculate only the forward scattering amplitude of the quarkonium. In that quantity, all the final state emissions ($\tau > 0$) cancel, as was shown in Ref. [50]. This is not the case for the inclusive production cross section that we want to calculate here. All final state emissions have to be taken into account, as shown in Fig. 3. Also, since we are interested in gluon production, the momentum of gluon #2 is fixed. Therefore, since we are going to perform our calculations in transverse coordinate space, we have to keep the transverse coordinates of gluon #2 different on both sides of the cut. (To obtain the cross section, we will afterwards perform a Fourier transform into transverse momentum space.) Thus, the gluon's transverse coordinate is denoted by $\underline{x}_2$ to the left of the cut and $\underline{x}_{2'}$ to the right of the cut. Then the color "dipole" formed by, say, the lines 2, 2′, and $\tilde{0}$ in Fig. 3(a) would not be literally a dipole since one needs more than two transverse coordinates to describe it, but it would still have the color topology of a dipole and we will refer to it as a dipole below.

Let us start by analyzing the gluon production in Fig. 3(a). As was mentioned before, the softer gluon #1 can be emitted either off the color dipole formed by lines 0, 2, and 2′ or off dipole 2, 2′, $\tilde{0}$. In the following analysis, we will concentrate on the latter case of emission of gluon #1 in dipole 2, 2′, $\tilde{0}$. (A generalization to emission in dipole 0, 2, and 2′ is straightforward.) We will denote by $M_0(\underline{x}_2, \underline{x}_{2'}, \underline{x}_{\tilde{0}}; \underline{k}_1)$ the cross section of emission of a softer gluon #1 in dipole 2, 2′, $\tilde{0}$. Then dipole 0, 2, 2′ would not have gluon emissions in it, but it would still be able to interact with the target. Interactions of the target with line 0 would cancel due to real-virtual cancellations [17,23,48]. Interactions with lines 2 and 2′ do not cancel: instead, they are given by the S matrix of a 22′ quark dipole interacting with the target [23,51]. The S matrix is

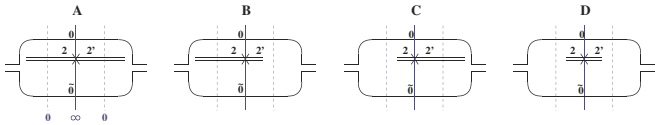

FIG. 3 (color online). All possible emission of the harder gluon #2 by the $q\bar{q}$ pair.

given by

$$S_0(\underline{x}_2, \underline{x}_{2'}) = 1 - N_0(\underline{x}_2, \underline{x}_{2'}), \tag{9}$$

where, in the Glauber-Mueller approximation, the forward scattering amplitude N_0 is [44]

$$N_0(\underline{x}_2, \underline{x}_{2'}) = 1 - e^{-x_{22'}^2 Q_{s0}^2 \ln(1/x_{22'}\Lambda)/4}, \tag{10}$$

where $x_{22'} = |\underline{x}_2 - \underline{x}_{2'}|$ and the quark saturation scale in the McLerran-Venugopalan model Q_{s0} [7,8] is given by (in the large-N_c limit)

$$Q_{s0}^2(\underline{b}) = 2\pi\alpha_s^2 \rho T(\underline{b}), \tag{11}$$

with ρ the atomic number density in the nucleus with atomic number A, $T(\underline{b})$ the nuclear profile function with $\underline{b} = (\underline{x}_2 + \underline{x}_{2'})/2$, and Λ some infrared cutoff.

In the diagram in Fig. 3(b), the softer gluon #1 cannot be emitted off gluon $2'$ in the complex conjugate amplitude: that would be suppressed due to the inverse ordering rule we derived in Sec. II A. Furthermore, if gluon $2'$ is emitted off the quark line 0, gluon #1 cannot be emitted in the dipole formed by lines 0 and $2'$ due to the same inverse ordering rule. Therefore, if gluon $2'$ is emitted off the quark line 0, gluon #1 can be emitted only by

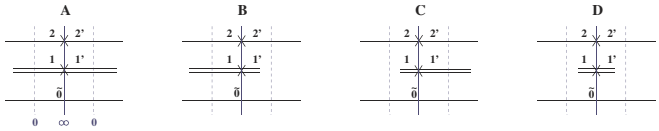

FIG. 4 (color online). All possible emissions of the softer gluon #1 by dipole $2, 2', \tilde{0}$.

dipole $0\tilde{0}$ in the complex conjugate amplitude. Therefore, the diagram in Fig. 3(b) would bring in a factor of $M_0(\underline{x}_2, \underline{x}_0, \underline{x}_{\tilde{0}}; \underline{k}_1)$ if gluon #1 is emitted in the lower dipole. In the same case, in the upper dipole, only dipole 02 would interact with the target bringing in a factor of $S_0(\underline{x}_0, \underline{x}_2)$. The diagram in Fig. 3(c) can be obtained from 3(b) by horizontal reflection, which can be accomplished by interchanging $\underline{x}_2 \leftrightarrow \underline{x}_{2'}$. Finally, a similar line of argument shows that the diagram in Fig. 3(d) brings in a factor of $M_0(\underline{x}_0, \underline{x}_0, \underline{x}_{\tilde{0}}; \underline{k}_1)$ if the gluon is emitted in the lower dipole.

Combining diagrams A–D in Fig. 3 and defining

$$\overline{\alpha}_s \equiv \frac{\alpha_s N_c}{\pi}, \tag{12}$$

we write

$$\begin{aligned}\frac{d\hat{\sigma}^{q\bar{q}A\to q\bar{q}GGX}}{d^2k_1 dy_1 d^2k_2 dy_2}(\underline{x}_{0\tilde{0}})|_{y_2 \gg y_1} = \frac{\overline{\alpha}_s}{(2\pi)^3}\int d^2B d^2x_2 d^2x_{2'} e^{-i\underline{k}_2\cdot\underline{x}_{22'}}\Bigg[\left(\frac{\underline{x}_{20}}{x_{20}^2} - \frac{\underline{x}_{2\tilde{0}}}{x_{2\tilde{0}}^2}\right)\left(\frac{\underline{x}_{2'0}}{x_{2'0}^2} - \frac{\underline{x}_{2'\tilde{0}}}{x_{2'\tilde{0}}^2}\right)M_0(\underline{x}_2, \underline{x}_{2'}, \underline{x}_{\tilde{0}}; \underline{k}_1)S_0(\underline{x}_2, \underline{x}_{2'}) \\ - \left(\frac{\underline{x}_{20}}{x_{20}^2} - \frac{\underline{x}_{2\tilde{0}}}{x_{2\tilde{0}}^2}\right)\frac{\underline{x}_{2'0}}{x_{2'0}^2}M_0(\underline{x}_2, \underline{x}_0, \underline{x}_{\tilde{0}}; \underline{k}_1)S_0(\underline{x}_0, \underline{x}_2) - \left(\frac{\underline{x}_{2'0}}{x_{2'0}^2} - \frac{\underline{x}_{2'\tilde{0}}}{x_{2'\tilde{0}}^2}\right)\frac{\underline{x}_{20}}{x_{20}^2}M_0(\underline{x}_0, \underline{x}_{2'}, \underline{x}_{\tilde{0}}; \underline{k}_1)S_0(\underline{x}_0, \underline{x}_{2'}) \\ + \frac{\underline{x}_{20}}{x_{20}^2}\frac{\underline{x}_{2'0}}{x_{2'0}^2}M_0(\underline{x}_0, \underline{x}_0, \underline{x}_{\tilde{0}}; \underline{k}_1) + (0 \leftrightarrow \tilde{0})\Bigg],\end{aligned} \tag{13}$$

where $\underline{B} = (\underline{x}_0 + \underline{x}_{\tilde{0}})/2$ is the impact parameter of the original dipole $0\tilde{0}$. The term $(0 \leftrightarrow \tilde{0})$ implies that we have to add the whole expression again, interchanging 0 and $\tilde{0}$ to account for the emission of gluon #1 from the top "dipole."

Now we have to calculate $M_0(\underline{x}_2, \underline{x}_{2'}, \underline{x}_{\tilde{0}}; \underline{k}_1)$. To do that, let us consider all possible emissions of gluon #1 in dipole $2, 2', \tilde{0}$ as shown in Fig. 4. The transverse coordinates of gluon #1 are $\underline{x}_1$ and $\underline{x}_{1'}$ to the left and to the right of the cut, correspondingly.

To calculate all the diagrams in Fig. 4, one has to use the rules of Sec. II A Let us illustrate the prescription for calculating these graphs for the fairly general case when gluon #1 is emitted off gluon #2 on both sides of the cut. Dipole $2, 2', \tilde{0}$ in Fig. 4(a) would then split into a dipole $1, 1', \tilde{0}$ and a quadrupole $2, 2', 1, 1'$. The interactions of line $\tilde{0}$ with the target cancel via real-virtual cancellations [17,48], thus reducing the interactions of dipole $1, 1', \tilde{0}$ to the interaction of a real dipole $1, 1'$ bringing in a factor of $S_0(\underline{x}_1, \underline{x}_{1'})$. The interaction of the quadrupole $2, 2', 1, 1'$ brings in a factor which we will denote $Q_0(\underline{x}_2, \underline{x}_{2'}, \underline{x}_1, \underline{x}_{1'})$. In the quasiclassical approximation of McLerran-Venugopalan model, this S matrix of the quadrupole interaction with the target Q_0 is calculated in the appendix, yielding (cf. [42])

$$\begin{aligned}Q_0(\underline{x}_2, \underline{x}_{2'}, \underline{x}_1, \underline{x}_{1'}) = e^{-[x_{21}^2 \ln(1/x_{21}\Lambda) + x_{2'1'}^2 \ln(1/x_{2'1'}\Lambda)]Q_{s0}^2/4} \\ + \frac{x_{22'}^2 \ln(1/x_{22'}\Lambda) + x_{11'}^2 \ln(1/x_{11'}\Lambda) - x_{21'}^2 \ln(1/x_{21'}\Lambda) - x_{2'1}^2 \ln(1/x_{2'1}\Lambda)}{x_{21}^2 \ln(1/x_{21}\Lambda) + x_{2'1'}^2 \ln(1/x_{2'1'}\Lambda) - x_{22'}^2 \ln(1/x_{22'}\Lambda) - x_{11'}^2 \ln(1/x_{11'}\Lambda)} \\ \times \left(e^{-[x_{21}^2 \ln(1/x_{21}\Lambda) + x_{2'1'}^2 \ln(1/x_{2'1'}\Lambda)]Q_{s0}^2/4} - e^{-[x_{11'}^2 \ln(1/x_{11'}\Lambda) + x_{22'}^2 \ln(1/x_{22'}\Lambda)]Q_{s0}^2/4}\right).\end{aligned} \tag{14}$$

As one can see from Eq. (14), $Q_0(\underline{x}_2, \underline{x}_2, \underline{x}_1, \underline{x}_1) = 1$, which is what one would expect due to real-virtual cancellations [17,23,48]. One can also check that

$$Q_0(\underline{x}_2, \underline{x}_{2'}, \underline{x}_1, \underline{x}_1) = e^{-x_{22'}^2 \ln(1/x_{22'}\Lambda) Q_{s0}^2/4}, \tag{15}$$

corresponding to the S matrix of the interaction of dipole $22'$ with the target. (Interactions with line 1 cancel again due to real-virtual cancellations if we put $\underline{x}_1 = \underline{x}_{1'}$.)

Now let us evaluate the graph in Fig. 4(b) for the same case of gluon #1 being emitted off gluon #2 on both sides of the cut. In the top dipole, interactions can take place only to the left of the cut, giving a factor of $S_0(\underline{x}_2, \underline{x}_1)$. In the bottom dipole, the interactions with line $\tilde{0}$ cancel, leaving only dipole $12'$ to interact with the target, which brings in a factor of $S_0(\underline{x}_1, \underline{x}_{2'})$. The diagram in Fig. 4(c) is evaluated in a similar way, yielding a factor of $S_0(\underline{x}_{2'}, \underline{x}_{1'}) S_0(\underline{x}_2, \underline{x}_{1'})$. Finally, in the diagram in Fig. 4(d), only the lower dipole can interact with the target, giving a factor of $S_0(\underline{x}_2, \underline{x}_{2'})$.

Combining the factors calculated above for diagrams A–D in Fig. 4, putting in the contribution of gluon emission, and summing over all possible connections of gluon #1 to lines 2, 2′, and 1, we obtain

$$\begin{aligned} M_0(\underline{x}_2, \underline{x}_{2'}, \underline{x}_{\tilde{0}}, \underline{k}_1) = \frac{\overline{\alpha}_s}{(2\pi)^3} \int d^2x_1 d^2x_{1'} e^{-i\underline{k}_1 \cdot \underline{x}_{11'}} \Bigg\{ & \frac{\underline{x}_{12}}{x_{12}^2} \frac{\underline{x}_{1'2'}}{x_{1'2'}^2} [Q_0(\underline{x}_2, \underline{x}_{2'}, \underline{x}_1, \underline{x}_{1'}) S_0(\underline{x}_1, \underline{x}_{1'}) + S_0(\underline{x}_2, \underline{x}_{2'}) \\ & - S_0(\underline{x}_2, \underline{x}_1) S_0(\underline{x}_1, \underline{x}_{2'}) - S_0(\underline{x}_{2'}, \underline{x}_{1'}) S_0(\underline{x}_2, \underline{x}_{1'})] + \frac{\underline{x}_{1\tilde{0}}}{x_{1\tilde{0}}^2} \frac{\underline{x}_{1'\tilde{0}}}{x_{1'\tilde{0}}^2} [Q_0(\underline{x}_2, \underline{x}_{2'}, \underline{x}_1, \underline{x}_{1'}) S_0(\underline{x}_1, \underline{x}_{1'}) \\ & + S_0(\underline{x}_2, \underline{x}_{2'}) - Q_0(\underline{x}_2, \underline{x}_{2'}, \underline{x}_1, \underline{x}_{\tilde{0}}) S_0(\underline{x}_1, \underline{x}_{\tilde{0}}) - Q_0(\underline{x}_2, \underline{x}_{2'}, \underline{x}_{\tilde{0}}, \underline{x}_{1'}) S_0(\underline{x}_{\tilde{0}}, \underline{x}_{1'})] \\ & - \frac{\underline{x}_{12}}{x_{12}^2} \frac{\underline{x}_{1'\tilde{0}}}{x_{1'\tilde{0}}^2} [Q_0(\underline{x}_2, \underline{x}_{2'}, \underline{x}_1, \underline{x}_{1'}) S_0(\underline{x}_1, \underline{x}_{1'}) + S_0(\underline{x}_2, \underline{x}_{\tilde{0}}) S_0(\underline{x}_{2'}, \underline{x}_{\tilde{0}}) - Q_0(\underline{x}_2, \underline{x}_{2'}, \underline{x}_1, \underline{x}_{\tilde{0}}) S_0(\underline{x}_1, \underline{x}_{\tilde{0}}) \\ & - S_0(\underline{x}_2, \underline{x}_{1'}) S_0(\underline{x}_{2'}, \underline{x}_{1'})] - \frac{\underline{x}_{1\tilde{0}}}{x_{1\tilde{0}}^2} \frac{\underline{x}_{1'2'}}{x_{1'2'}^2} [Q_0(\underline{x}_2, \underline{x}_{2'}, \underline{x}_1, \underline{x}_{1'}) S_0(\underline{x}_1, \underline{x}_{1'}) + S_0(\underline{x}_2, \underline{x}_{\tilde{0}}) S_0(\underline{x}_{2'}, \underline{x}_{\tilde{0}}) \\ & - S_0(\underline{x}_2, \underline{x}_1) S_0(\underline{x}_{2'}, \underline{x}_1) - Q_0(\underline{x}_2, \underline{x}_{2'}, \underline{x}_{\tilde{0}}, \underline{x}_{1'}) S_0(\underline{x}_{1'}, \underline{x}_{\tilde{0}})] \Bigg\}. \end{aligned} \tag{16}$$

Equations (1) and (13) together with Eqs. (9), (10), (14), and (16) give us the two-gluon inclusive production cross section for DIS on a nucleus including all the quasiclassical multiple rescatterings in the large-N_c approximation. It is the main result of this section.

III. TWO-GLUON PRODUCTION INCLUDING QUANTUM EVOLUTION

In this section, our goal is to include the effects of nonlinear small-x quantum evolution of Ref. [9] into the quasiclassical expression (13) for an inclusive two-gluon production cross section. We will begin by reviewing the nonlinear evolution equation and its application to single inclusive gluon production. We will proceed by deriving the expression generalizing Eq. (13) by including the nonlinear evolution [9] in it. We will conclude by verifying that the obtained expression matches the standard k_T-factorization result [37] at the leading-twist level.

A. Brief review of small-x evolution and single gluon production

To include the effects of small-x evolution in the dipole S matrix, one first defines the S matrix for a quark dipole $0\tilde{0}$ having rapidity Y with respect to the target as

$$S(\underline{x}_0, \underline{x}_{\tilde{0}}, Y) = 1 - N(\underline{x}_0, \underline{x}_{\tilde{0}}, Y), \tag{17}$$

where the forward scattering amplitude has to be determined from the nonlinear evolution equation [9]

$$\begin{aligned} N(\underline{x}_0, \underline{x}_{\tilde{0}}, Y) = {} & N_0(\underline{x}_0, \underline{x}_{\tilde{0}}) e^{-2\overline{\alpha}_s \ln(x_{0\tilde{0}}/\rho) Y} \\ & + \frac{\overline{\alpha}_s}{2\pi} \int_0^Y dy e^{-2\overline{\alpha}_s \ln(x_{0\tilde{0}}/\rho)(Y-y)} \\ & \times \int_\rho d^2x_2 \frac{x_{0\tilde{0}}^2}{x_{20}^2 x_{2\tilde{0}}^2} [N(\underline{x}_0, \underline{x}_2, y) + N(\underline{x}_2, \underline{x}_{\tilde{0}}, y) \\ & - N(\underline{x}_0, \underline{x}_2, y) N(\underline{x}_2, \underline{x}_{\tilde{0}}, y)], \end{aligned} \tag{18}$$

with the initial condition given by Eq. (10) and ρ being an ultraviolet cutoff [49]. The evolution Eq. (18) resums all powers of leading logarithms of center of mass energy $\alpha_s Y$ and all multiple interactions with the target, which brings in powers of $\alpha_s^2 A^{1/3}$, with A the atomic number of the nucleus [8,17,20,48].

Equation (18) is derived in Ref. [9] by resumming a cascade of gluons in the incoming $q\bar{q}$ wave function, which in the large-N_c limit turns into a cascade of color dipoles. The emissions are similar to the ones we considered in Sec. II A for the early times preceding the interaction. The difference is that in Ref. [9] one resums emissions to all orders, without limiting oneself to just

two gluons. At the leading logarithmic level, the contribution of this gluonic (dipole) cascade to the S matrix of the dipole-nucleus scattering is given by the solution of Eq. (18). However, one can use this cascade to construct other useful observables.

In Ref. [23] it was shown that an inclusive gluon production cross section in a dipole-nucleus scattering is given by the following formula:

$$\frac{d\sigma^{q\bar{q}A\to q\bar{q}GX}}{d^2k\,dy}(\underline{x}_{0\tilde{0}}) = \int d^2B\, n_1(\underline{x}_0, \underline{x}_{\tilde{0}}, Y; \underline{x}_1, \underline{x}_2, y) \times d^2x_1 d^2x_2\, s(\underline{x}_1, \underline{x}_2, \underline{k}, y), \tag{19}$$

where we defined

$$s(\underline{x}_1, \underline{x}_2, \underline{k}, y) \equiv \frac{\overline{\alpha}_s}{(2\pi)^3} \int d^2z_1 d^2z_2 e^{-i\underline{k}\cdot(\underline{z}_1-\underline{z}_2)} \sum_{i,j=1}^{2} (-1)^{i+j} \frac{\underline{z}_1-\underline{x}_i}{|\underline{z}_1-\underline{x}_i|^2} \frac{\underline{z}_2-\underline{x}_j}{|\underline{z}_2-\underline{x}_j|^2} [N_G(\underline{z}_1, \underline{x}_j, y) + N_G(\underline{z}_2, \underline{x}_i, y) - N_G(\underline{z}_1, \underline{z}_2, y) - N_G(\underline{x}_i, \underline{x}_j, y)] \tag{20}$$

in terms of the forward scattering amplitude of the adjoint (gluon) dipole, which in the large-N_c limit can be easily expressed in terms of the forward amplitude of the fundamental (quark) dipole

$$N_G(\underline{x}_0, \underline{x}_1, y) = 2N(\underline{x}_0, \underline{x}_1, y) - N^2(\underline{x}_0, \underline{x}_1, y). \tag{21}$$

In Eq. (19) the quantity $n_1(\underline{x}_0, \underline{x}_{\tilde{0}}, Y; \underline{x}_1, \underline{x}_2, y)$ has the meaning of the probability of finding a dipole 12 at rapidity y in the original dipole $0\tilde{0}$ having rapidity Y [49]. It obeys the following equation [49]:

$$n_1(\underline{x}_0, \underline{x}_{\tilde{0}}, Y; \underline{x}_1, \underline{x}_{\tilde{1}}, y) = \delta^2(\underline{x}_0-\underline{x}_1)\delta(\underline{x}_{\tilde{0}}-\underline{x}_{\tilde{1}}) e^{-2\overline{\alpha}_s \ln(x_{0\tilde{0}}/\rho)(Y-y)} + \frac{\overline{\alpha}_s}{2\pi} \int_y^Y dy' e^{-2\overline{\alpha}_s \ln(x_{0\tilde{0}}/\rho)(Y-y')} \times \int_\rho d^2x_2 \frac{x_{0\tilde{0}}^2}{x_{20}^2 x_{2\tilde{0}}^2} [n_1(\underline{x}_0, \underline{x}_2, y'; \underline{x}_1, \underline{x}_{\tilde{1}}, y) + n_1(\underline{x}_2, \underline{x}_{\tilde{0}}, y'; \underline{x}_1, \underline{x}_{\tilde{1}}, y)], \tag{22}$$

which is the linear part of the dipole evolution Eq. (18) equivalent to the BFKL equation [30].

The quantity $s(\underline{x}_1, \underline{x}_2, \underline{k}, y)$ in Eq. (19) is the cross section for single gluon production by dipole 12 scattering on a nucleus at rapidity y with the emitted gluon being the first (hardest) gluon in the gluonic (dipole) cascade developed by the incoming dipole 12. Then Eq. (19) has a simple physical meaning: it convolutes the probability of finding a dipole in the initial onium wave function which would emit the gluon with the probability of the gluon emission by this dipole.

To recover the quasiclassical result for single gluon production [17], one has to put $Y = y = 0$ on the right-hand side of Eq. (19). That would effectively turn off the quantum evolution, giving

$$\frac{d\sigma^{q\bar{q}A\to q\bar{q}GX}}{d^2k\,dy}(\underline{x}_{0\tilde{0}}) = \int d^2B\, s(\underline{x}_0, \underline{x}_{\tilde{0}}, \underline{k}, 0) = \int d^2B d^2z_1 d^2z_2 e^{-i\underline{k}\cdot(\underline{z}_1-\underline{z}_2)} \sum_{i,j=1}^{2} (-1)^{i+j} \frac{\underline{z}_1-\underline{x}_i}{|\underline{z}_1-\underline{x}_i|^2} \frac{\underline{z}_2-\underline{x}_j}{|\underline{z}_2-\underline{x}_j|^2} (e^{-(\underline{x}_i-\underline{x}_j)^2 Q_{s0}^2 \ln(1/|\underline{x}_i-\underline{x}_j|\Lambda)/2} - e^{-(\underline{z}_1-\underline{x}_j)^2 Q_{s0}^2 \ln(1/|\underline{z}_1-\underline{x}_j|\Lambda)/2} - e^{-(\underline{z}_2-\underline{x}_i)^2 Q_{s0}^2 \ln(1/|\underline{z}_2-\underline{x}_i|\Lambda)/2} + e^{-(\underline{z}_1-\underline{z}_2)^2 Q_{s0}^2 \ln(1/|\underline{z}_1-\underline{z}_2|\Lambda)/2}), \tag{23}$$

which is the quasiclassical gluon production cross section found in Refs. [17–20].

If the evolution Eq. (18) is pictured as resumming the so-called "fan" diagrams in dipole-nucleus scattering [4,5], then the single inclusive gluon production cross section would correspond to diagrams such as the one shown in Fig. 5. There, the produced gluon, which is denoted by the cross, can be emitted only from the top ladder in the diagram. As it turned out, emissions from all other (lower) ladders cancel [23], in agreement with expectations of the AGK cutting rules [43] (see also [24]). Thus, the evolution between the projectile and the produced gluon is just a linear BFKL evolution, as we can see in Eq. (22). The evolution between the produced gluon and the target is the full nonlinear evolution given by Eq. (18), as can be seen from Eq. (19).

Before concluding the subsection, let us define another useful quantity. Following Ref. [49], let

$$n_2(\underline{x}_0, \underline{x}_{\tilde{0}}, Y; \underline{x}_1, \underline{x}_{\tilde{1}}, y_1, \underline{x}_2, \underline{x}_{\tilde{2}}, y_2)$$

be the probability of finding dipoles $1\tilde{1}$ and $2\tilde{2}$ with rapidities y_1 and y_2, correspondingly, in the original dipole $0\tilde{0}$ having rapidity Y. This quantity obeys the following evolution equation [49]:

$$n_2(\underline{x}_0, \underline{x}_{\tilde{0}}, Y; \underline{x}_1, \underline{x}_{\tilde{1}}, y_1, \underline{x}_2, \underline{x}_{\tilde{2}}, y_2) = \frac{\overline{\alpha}_s}{2\pi} \int_{\max\{y_1,y_2\}}^{Y} dy e^{-2\overline{\alpha}_s \ln(x_{0\tilde{0}}/\rho)(Y-y)} \int_\rho d^2x_3 \frac{x_{0\tilde{0}}^2}{x_{30}^2 x_{3\tilde{0}}^2}$$
$$\times [n_1(\underline{x}_0, \underline{x}_3, y; \underline{x}_1, \underline{x}_{\tilde{1}}, y_1) n_1(\underline{x}_3, \underline{x}_{\tilde{0}}, y; \underline{x}_2, \underline{x}_{\tilde{2}}, y_2) + n_1(\underline{x}_0, \underline{x}_3, y; \underline{x}_2, \underline{x}_{\tilde{2}}, y_2)$$
$$\times n_1(\underline{x}_3, \underline{x}_{\tilde{0}}, y; \underline{x}_1, \underline{x}_{\tilde{1}}, y_1) + n_2(\underline{x}_0, \underline{x}_3, y; \underline{x}_1, \underline{x}_{\tilde{1}}, y_1, \underline{x}_2, \underline{x}_{\tilde{2}}, y_2)$$
$$+ n_2(\underline{x}_3, \underline{x}_{\tilde{0}}, y; \underline{x}_1, \underline{x}_{\tilde{1}}, y_1, \underline{x}_2, \underline{x}_{\tilde{2}}, y_2)], \tag{24}$$

which is linear and can be solved after one finds n_1 from Eq. (22).

B. Two-gluon inclusive cross section with quantum evolution

Now we have all the essential ingredients necessary to include quantum evolution effects in Eq. (13). Similarly to the analysis carried out in Ref. [23], we will separate all the gluons into the ones which are harder (have higher rapidity with respect to the target) than the harder of the two gluons with rapidities y_1 and y_2 that are going to be produced and into the ones which are softer (have lower rapidity) than the gluon y_2 ($y_2 \gg y_1$).

Similarly to the analysis of Sec. IIIA in Ref. [23], one can easily conclude that all of the harder gluons can be emitted only at early ($\tau < 0$) times both in the amplitude and in the complex conjugate amplitude. Because of the ordering rule from Sec. II A of this paper, this implies that these harder gluons have to be emitted before gluons #2 and #1. Therefore, we have to distinguish two important cases:

A. Gluons #2 and #1 are emitted in two different dipoles created by the evolution due to emission of gluons which are harder than either gluon #2 or gluon #1.

B. Gluon #2 is emitted in a dipole created by the evolution consisting of emissions of harder gluons. Gluon #1 is emitted either by one of the dipoles adjacent to gluon #2 (as was studied in Fig. 4) or in a dipole generated by evolution inside one of these adjacent dipoles.

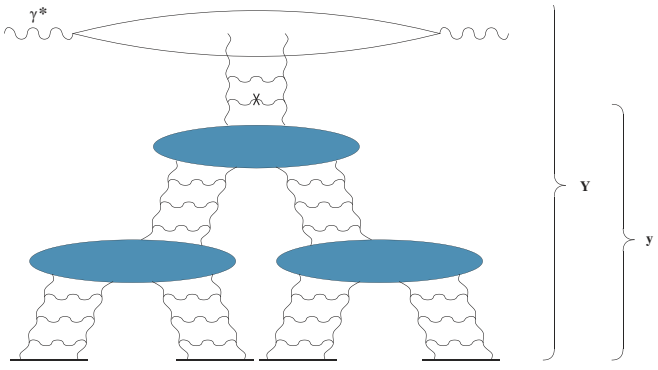

FIG. 5 (color online). Feynman diagram corresponding to single gluon production cross section given by Eq. (19). The emitted gluon is denoted by the cross.

Case A is relatively straightforward. Quantum evolution creating two dipoles of given sizes and rapidities at times $\tau < 0$ is included in the quantity n_2 from Eq. (24). Emission of each of the gluons #1 and #2 in two independent dipoles is equivalent to the same problem of a single inclusive gluon emission in a dipole-nucleus collision as considered in Sec. III A and is described by the quantity s from Eq. (20), which also includes all the successive evolution generated through emissions of gluons softer than either #1 or #2 [23]. Therefore, the contribution of case A to double gluon production can be written as

$$\int d^2B n_2(\underline{x}_0, \underline{x}_{\tilde{0}}, Y; \underline{x}_1, \underline{x}_{\tilde{1}}, y_1, \underline{x}_2, \underline{x}_{\tilde{2}}, y_2) d^2x_1 d^2x_{\tilde{1}} d^2x_2 d^2$$
$$\times x_{\tilde{2}} s(\underline{x}_1, \underline{x}_{\tilde{1}}, \underline{k}_1, y_1) s(\underline{x}_2, \underline{x}_{\tilde{2}}, \underline{k}_2, y_2), \tag{25}$$

with $\underline{B} = (\underline{x}_0 + \underline{x}_{\tilde{0}})/2$ as before.

Contribution of case B is somewhat more complicated. The probability of finding an early time ($\tau < 0$) dipole in the original onium in which gluon #2 is emitted is described by the quantity n_1 from Eq. (22). Emission of gluon #2 is then described by the diagrams of Fig. 3 and, equivalently, by Eq. (13). The only difference is that now we have to include quantum evolution in the quantity M_0 and in the S matrix S_0. The inclusion of evolution into the S matrix S_0 is accomplished in Eqs. (17) and (18). The inclusion of evolution into the quantity M_0 requires a separate diagrammatic analysis, shown in Fig. 6.

Let us first define a quantity $M(\underline{x}_2, \underline{x}_{2'}, \underline{x}_{\tilde{0}}, Y; \underline{k}_1, y_1)$, which by analogy with M_0 has a physical meaning of an inclusive cross section of producing a gluon with transverse momentum $\underline{k}_1$ and rapidity y_1 in dipole $2, 2', \tilde{0}$ having rapidity Y. To write an evolution equation for $M(\underline{x}_2, \underline{x}_{2'}, \underline{x}_{\tilde{0}}, Y; \underline{k}_1, y_1)$, one has to analyze a single step of small-x evolution for this quantity. All the important gluon emissions in dipole $2, 2', \tilde{0}$ are shown in Fig. 6. We start the analysis with the diagram in Fig. 6(a). Emitting gluon #4 splits the original dipole $2, 2', \tilde{0}$ into a dipole $2, 2', 4$ and a dipole $4\tilde{0}$. Then gluon #1 can be emitted in dipole $2, 2', 4$, which would bring in a factor of

$$M(\underline{x}_2, \underline{x}_{2'}, \underline{x}_4, y; \underline{k}_1, y_1),$$

with y the rapidity of gluon #4. In this case all interactions in dipole $4\tilde{0}$ cancel. Alternatively, gluon #1 can be emitted in dipole $4\tilde{0}$, which would bring in the familiar factor of

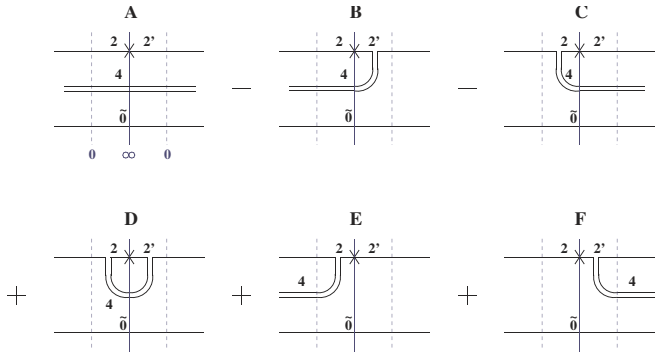

FIG. 6 (color online). Diagrams describing one step of evolution for M.

$$\int d^2x_a d^2x_b n_1(\underline{x}_4, \underline{x}_{\tilde{0}}, y; \underline{x}_a, \underline{x}_b, y_1) s(\underline{x}_a, \underline{x}_b, \underline{k}_1, y_1)$$

from Eq. (19) describing a single inclusive gluon production in a dipole-nucleus scattering. In this second case, interactions of dipole $2, 2', 4$ with the target would not completely cancel. Instead, they would bring in a factor of $S(\underline{x}_2, \underline{x}_{2'}, y) = 1 - N(\underline{x}_2, \underline{x}_{2'}, y)$, corresponding to interaction of dipole $22'$ with the target.

In the diagram shown in Fig. 6(b), the interaction of gluon #4 with line $\tilde{0}$ to the right of the cut gets canceled by the diagram similar to the one in Fig. 6(e) but with gluon #4 connecting to line $\tilde{0}$ instead of line 2 to the right of the cut [50]. Therefore, gluon #4 interacts only with line $2'$ on the right-hand side of Fig. 6(b) and only with line 2 on the right-hand side of Fig. 6(e). Because of the inverse ordering rule for late-time emissions from Sec. II A, gluon #1 cannot be emitted in dipole 24 in graph B of Fig. 6. [In Fig. 6(e) dipole 24 is not present in the final state and cannot contribute to gluon production.] Therefore, in both graphs B and E dipole 24 brings in only a factor of $S(\underline{x}_2, \underline{x}_4, y) = 1 - N(\underline{x}_2, \underline{x}_4, y)$ into the evolution equation we are constructing. The other dipole $4, 2', \tilde{0}$ would then bring in a factor of

$$M(\underline{x}_4, \underline{x}_{2'}, \underline{x}_{\tilde{0}}, y; \underline{k}_1, y_1).$$

Diagrams C and F can be obtained from B and E by interchanging $2 \leftrightarrow 2'$. Finally, in diagram D interactions of gluon #4 with line $\tilde{0}$ cancel due to real-virtual cancellations of Ref. [50] that we have just employed in graphs B and E. The remaining interaction with lines 2 and $2'$ shown in Fig. 6(d) does not split dipole $2, 2', \tilde{0}$. Because of the inverse ordering rule of Sec. II A, there will be no softer gluon emissions in dipole $2, 2'4$, such that all subsequent evolution will take place only in dipole $2, 2', \tilde{0}$. Therefore, diagram D contributes only to virtual corrections, along with the usual virtual corrections at $\tau < 0$ in dipoles $2\tilde{0}$ and $2'\tilde{0}$.

Combining the contributions of all diagrams in Fig. 6, we write the following evolution equation:

$$\begin{aligned} M(\underline{x}_2, \underline{x}_{2'}, \underline{x}_{\tilde{0}}, Y; \underline{k}_1, y_1) = {} & e^{-\overline{\alpha}_s \ln(x_{2\tilde{0}} x_{2'\tilde{0}} x_{22'}/\rho^3)(Y-y_1)} d(\underline{x}_2, \underline{x}_{2'}, \underline{x}_{\tilde{0}}, \underline{k}_1, y_1) + \frac{\overline{\alpha}_s}{2\pi} \int d^2x_4 \int_{y_1}^{Y} dy e^{-\overline{\alpha}_s \ln(x_{2\tilde{0}} x_{2'\tilde{0}} x_{22'}/\rho^3)(Y-y)} \\ & \times \left\{ \left(\frac{\underline{x}_{42}}{x_{42}^2} - \frac{\underline{x}_{4\tilde{0}}}{x_{4\tilde{0}}^2} \right) \left(\frac{\underline{x}_{42'}}{x_{42'}^2} - \frac{\underline{x}_{4\tilde{0}}}{x_{4\tilde{0}}^2} \right) \right. \Bigg[M(\underline{x}_2, \underline{x}_{2'}, \underline{x}_4, y; \underline{k}_1, y_1) + \int d^2x_a d^2x_b n_1(\underline{x}_4, \underline{x}_{\tilde{0}}, y; \underline{x}_a, \underline{x}_b, y_1) \\ & \times s(\underline{x}_a, \underline{x}_b, \underline{k}_1, y_1)(1 - N(\underline{x}_2, \underline{x}_{2'}, y)) \Bigg] - \left(\frac{\underline{x}_{42}}{x_{42}^2} - \frac{\underline{x}_{4\tilde{0}}}{x_{4\tilde{0}}^2} \right) \left(\frac{\underline{x}_{42'}}{x_{42'}^2} - \frac{\underline{x}_{42}}{x_{42}^2} \right) M(\underline{x}_4, \underline{x}_{2'}, \underline{x}_{\tilde{0}}, y; \underline{k}_1, y_1) \\ & \times [1 - N(\underline{x}_2, \underline{x}_4, y)] - \left(\frac{\underline{x}_{42}}{x_{42}^2} - \frac{\underline{x}_{42'}}{x_{42'}^2} \right) \left(\frac{\underline{x}_{42'}}{x_{42'}^2} - \frac{\underline{x}_{4\tilde{0}}}{x_{4\tilde{0}}^2} \right) M(\underline{x}_2, \underline{x}_4, \underline{x}_{\tilde{0}}, y; \underline{k}_1, y_1)[1 - N(\underline{x}_{2'}, \underline{x}_4, y)] \Bigg\}. \end{aligned} \quad (26)$$

The only thing left to do to complete our analysis is to determine the initial condition for the evolution Eq. (26), which we denoted $d(\underline{x}_2, \underline{x}_{2'}, \underline{x}_{\tilde{0}}, \underline{k}_1, y_1)$. This quantity is the gluon production cross section in the scattering of a dipole $2, 2', \tilde{0}$ on a nucleus with the small-x quantum evolution included, in which the emitted gluon $(\underline{k}_1, y_1)$ is the first (hardest) gluon in the gluonic cascade resumming the quantum evolution of Eq. (18). Since the emission diagrams are the same as in Fig. 4, the quantity $d(\underline{x}_2, \underline{x}_{2'}, \underline{x}_{\tilde{0}}, \underline{k}_1, y_1)$ should be given by the expression similar to Eq. (16), where the dipole and quadrupole S matrices S_0 and Q_0 have to be replaced by their evolved values. We, therefore, write

$$d(\underline{x}_2,\underline{x}_{2'},\underline{x}_{\tilde{0}},\underline{k}_1,y_1)=\frac{\overline{\alpha}_s}{(2\pi)^3}\int d^2x_1 d^2x_{1'}e^{-i\underline{k}_1\cdot\underline{x}_{11'}}\left\{\frac{\underline{x}_{12}}{x_{12}^2}\frac{\underline{x}_{1'2'}}{x_{1'2'}^2}[Q(\underline{x}_2,\underline{x}_{2'},\underline{x}_1,\underline{x}_{1'},y_1)S(\underline{x}_1,\underline{x}_{1'},y_1)+S(\underline{x}_2,\underline{x}_{2'},y_1)\right.$$
$$-S(\underline{x}_2,\underline{x}_1,y_1)S(\underline{x}_1,\underline{x}_{2'},y_1)-S(\underline{x}_{2'},\underline{x}_{1'},y_1)S(\underline{x}_2,\underline{x}_{1'},y_1)]+\frac{\underline{x}_{1\tilde{0}}}{x_{1\tilde{0}}^2}\frac{\underline{x}_{1'\tilde{0}}}{x_{1'\tilde{0}}^2}[Q(\underline{x}_2,\underline{x}_{2'},\underline{x}_1,\underline{x}_{1'},y_1)S(\underline{x}_1,\underline{x}_{1'},y_1)$$
$$+S(\underline{x}_2,\underline{x}_{2'},y_1)-Q(\underline{x}_2,\underline{x}_{2'},\underline{x}_1,\underline{x}_{\tilde{0}},y_1)S(\underline{x}_1,\underline{x}_{\tilde{0}},y_1)-Q(\underline{x}_2,\underline{x}_{2'},\underline{x}_{\tilde{0}},\underline{x}_{1'},y_1)S(\underline{x}_{\tilde{0}},\underline{x}_{1'},y_1)]$$
$$-\frac{\underline{x}_{12}}{x_{12}^2}\frac{\underline{x}_{1'\tilde{0}}}{x_{1'\tilde{0}}^2}[Q(\underline{x}_2,\underline{x}_{2'},\underline{x}_1,\underline{x}_{1'},y_1)S(\underline{x}_1,\underline{x}_{1'},y_1)+S(\underline{x}_2,\underline{x}_{\tilde{0}},y_1)S(\underline{x}_{2'},\underline{x}_{\tilde{0}},y_1)-Q(\underline{x}_2,\underline{x}_{2'},\underline{x}_1,\underline{x}_{\tilde{0}},y_1)S(\underline{x}_1,\underline{x}_{\tilde{0}},y_1)$$
$$-S(\underline{x}_2,\underline{x}_{1'},y_1)S(\underline{x}_{2'},\underline{x}_{1'},y_1)]-\frac{\underline{x}_{1\tilde{0}}}{x_{1\tilde{0}}^2}\frac{\underline{x}_{1'2'}}{x_{1'2'}^2}[Q(\underline{x}_2,\underline{x}_{2'},\underline{x}_1,\underline{x}_{1'},y_1)S(\underline{x}_1,\underline{x}_{1'},y_1)+S(\underline{x}_2,\underline{x}_{\tilde{0}},y_1)S(\underline{x}_{2'},\underline{x}_{\tilde{0}},y_1)$$
$$\left.-S(\underline{x}_2,\underline{x}_1,y_1)S(\underline{x}_{2'},\underline{x}_1,y_1)-Q(\underline{x}_2,\underline{x}_{2'},\underline{x}_{\tilde{0}},\underline{x}_{1'},y_1)S(\underline{x}_{1'},\underline{x}_{\tilde{0}},y_1)]\right\}. \tag{27}$$

Indeed, $S(\underline{x}_1,\underline{x}_{1'},y_1)$ in Eq. (27) is given by Eqs. (17) and (18). The reason why inclusion of evolution just corresponds to replacing the Glauber-Mueller expression (9) for S_0 by the fully evolved Eq. (17) has been discussed before in Ref. [23]. It was observed there that real-virtual cancellations for the gluon emissions contributing to the dipole evolution discussed in Ref. [50] act very much like the real-virtual cancellations for Glauber-Mueller multiple rescatterings [17]. Namely, if interactions of exchanged Coulomb gluons with a given quark line cancel in the multiple rescattering (Glauber-Mueller) picture, then emissions of an s-channel gluon by the same quark line at early and late times on both sides of the cut would also cancel [50]. One can show that interactions with quark and gluon lines that contribute in the multiple rescattering case would also contribute in the case of evolution. In the end, one concludes that inclusion of quantum evolution can be accomplished by replacing S_0 from Eqs. (9) and (10) by S from Eqs. (17) and (18) [23].

To calculate $Q(\underline{x}_2,\underline{x}_{2'},\underline{x}_1,\underline{x}_{1'},y_1)$, we have to write an evolution equation for the S matrix of the evolution of quadrupole $2, 2', 1, 1'$. An evolution equation involving a color quadrupole was derived before in Ref. [50] to reproduce the Bartels-Jaroszewicz-Kwiecinski-Praszalowicz (BJKP) equation [52] for four Reggeons in the framework of the dipole model [49]. The equation derived in Ref. [50] corresponds to off-forward evolution for dipoles in the presence of a single quadrupole, with all the evolution included in the dipoles. Therefore, it should not be compared to the equation we are about to write, since we are interested in the evolution inside the quadrupole.

We are going to derive an evolution equation for the quadrupole S matrix $Q(\underline{x}_2,\underline{x}_{2'},\underline{x}_1,\underline{x}_{1'},y_1)$ including all the nonlinear evolution effects. The initial condition for evolution of $Q(\underline{x}_2,\underline{x}_{2'},\underline{x}_1,\underline{x}_{1'},y_1)$ is given by Eq. (14). To write one step of the evolution, we first redraw the quadrupole as shown in Fig. 7. Instead of the amplitude squared pictured on the left in Fig. 7, we will use a form of quadrupole cross section similar to the forward amplitude shown on the right in Fig. 7. Obviously, the diagram on the right in Fig. 7 preserves the color structure of the quadrupole. All the interactions with the target in the graph on the left happen along the dashed lines at time $\tau = 0$. On the right in Fig. 7, we merge two dashed lines from the graph on the left into one dashed line with interactions in it. This way, a real interaction with a nucleon where a single gluon is exchanged in each of the dashed lines in the left graph in Fig. 7 becomes a two-gluon exchange (diffractive) interaction in the dashed line in the graph on the right in Fig. 7. Again, the picture is similar to the forward amplitude calculation.

One step of the quadrupole evolution in the representation in Fig. 7 is shown in Fig. 8. The step consists of an emission of a single gluon #3. For instance, in Fig. 8(a) gluon #3 splits the original quadrupole $2, 2', 1, 1'$ into a quadrupole $3, 2', 1, 1'$ and a dipole 23. Figure 8(b) gives a similar contribution. In Figs. 8(c)–8(f) we drew the gluon #3 line as disconnected at the dashed line: the gluon line is indeed implied to be connected and continuous. The disconnected line is just a notation which we borrowed from Ref. [50] for, say, a gluon emitted in dipole 21 and absorbed in dipole $11'$ in Fig. 8(c). However, when connecting the two parts of the gluon #3 line in Figs. 8(c)–8(f) one has to be careful to pick up the leading large-N_c contribution. For instance, in Fig. 8(c) the leading term consists of gluon #3 splitting

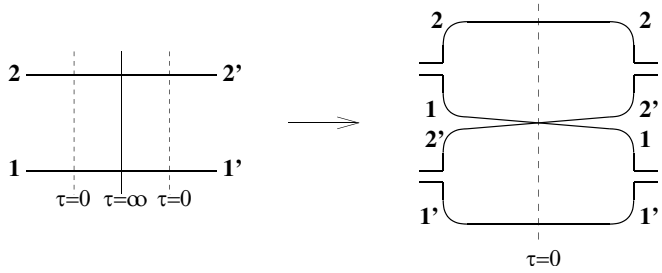

FIG. 7. Redrawing the quadrupole interaction amplitude in the form convenient for including quantum evolution (see text).

the original quadrupole $2, 2', 1, 1'$ into a dipole 31 and a quadrupole $2, 3, 1', 2'$. The dominant contribution of Fig. 8(e) consists of gluon #3 splitting the quadrupole $2, 2', 1, 1'$ into dipoles $2, 2', 3$ and $1, 1', 3$, in which interactions with line 3 cancel due to real-virtual cancellations. Leading terms for other graphs in Fig. 8 can be obtained in similar ways. Combining them with virtual corrections yields

$$
\begin{aligned}
Q(\underline{x}_2, \underline{x}_{2'}, \underline{x}_1, \underline{x}_{1'}, y_1) = {} & e^{-\overline{\alpha}_s \ln(x_{21}x_{2'1'}/x_{22'}x_{11'}/\rho^4)y_1} Q_0(\underline{x}_2, \underline{x}_{2'}, \underline{x}_1, \underline{x}_{1'}) + \frac{\overline{\alpha}_s}{2\pi}\int_0^{y_1} dy e^{-\overline{\alpha}_s \ln(x_{21}x_{2'1'}/x_{22'}x_{11'}/\rho^4)(y_1-y)} \\
& \times \int d^2x_3 \Bigg\{ \left(\frac{\underline{x}_{32}}{x_{32}^2} - \frac{\underline{x}_{31}}{x_{31}^2}\right)\left(\frac{\underline{x}_{32}}{x_{32}^2} - \frac{\underline{x}_{32'}}{x_{32'}^2}\right) S(\underline{x}_2, \underline{x}_3, y) Q(\underline{x}_3, \underline{x}_{2'}, \underline{x}_1, \underline{x}_{1'}, y) + \left(\frac{\underline{x}_{32'}}{x_{32'}^2} - \frac{\underline{x}_{31'}}{x_{31'}^2}\right)\left(\frac{\underline{x}_{31}}{x_{31}^2} - \frac{\underline{x}_{31'}}{x_{31'}^2}\right) \\
& \times S(\underline{x}_3, \underline{x}_{1'}, y) Q(\underline{x}_2, \underline{x}_{2'}, \underline{x}_1, \underline{x}_3, y) - \left(\frac{\underline{x}_{32}}{x_{32}^2} - \frac{\underline{x}_{31}}{x_{31}^2}\right)\left(\frac{\underline{x}_{31}}{x_{31}^2} - \frac{\underline{x}_{31'}}{x_{31'}^2}\right) S(\underline{x}_3, \underline{x}_1, y) Q(\underline{x}_2, \underline{x}_{2'}, \underline{x}_3, \underline{x}_{1'}, y) \\
& - \left(\frac{\underline{x}_{32}}{x_{32}^2} - \frac{\underline{x}_{32'}}{x_{32'}^2}\right)\left(\frac{\underline{x}_{32'}}{x_{32'}^2} - \frac{\underline{x}_{31'}}{x_{31'}^2}\right) S(\underline{x}_3, \underline{x}_{2'}, y) Q(\underline{x}_2, \underline{x}_3, \underline{x}_1, \underline{x}_{1'}, y) + \left(\frac{\underline{x}_{32}}{x_{32}^2} - \frac{\underline{x}_{31}}{x_{31}^2}\right)\left(\frac{\underline{x}_{32'}}{x_{32'}^2} - \frac{\underline{x}_{31'}}{x_{31'}^2}\right) \\
& \times S(\underline{x}_2, \underline{x}_{2'}, y) S(\underline{x}_1, \underline{x}_{1'}, y) + \left(\frac{\underline{x}_{32}}{x_{32}^2} - \frac{\underline{x}_{32'}}{x_{32'}^2}\right)\left(\frac{\underline{x}_{31}}{x_{31}^2} - \frac{\underline{x}_{31'}}{x_{31'}^2}\right) S(\underline{x}_2, \underline{x}_1, y) S(\underline{x}_{2'}, \underline{x}_{1'}, y) \Bigg\}. \qquad (28)
\end{aligned}
$$

Note that due to real-virtual cancellations the last two terms in Eq. (28) corresponding to diagrams E and F in Fig. 8 contain only the dipole S matrices in them. The relative signs of various terms in Eq. (28) are easier to determine in the representation of the interaction on the left-hand side in Fig. 7, keeping in mind that gluon emissions at $\tau < 0$ and $\tau > 0$ come in with different signs.

As we have already mentioned, the linearized version of Eq. (28) [see Eq. (38) below] should be combined with Eq. (49) in Ref. [50] to complete the description of the BJKP evolution in the framework of the dipole model. By linearizing Eq. (28) we mean substituting $S = 1 - N$ in it [see Eq. (17)] while keeping only terms linear in Q and in N, i.e., neglecting products such as QN and NN. However, as was discussed in Ref. [50], the contribution of linearized Eq. (28) to BJKP evolution is likely to be small: as we will see in the next subsection, the linearized version of Eq. (28) is almost equivalent to the BFKL equation. Therefore, its solution is likely to grow with energy just like a single BFKL Pomeron, which is much slower than the double BFKL Pomeron exchange. On the other hand, a solution of the full BJKP evolution equation for four Reggeons presented in Ref. [53] has an intercept much smaller than that of a single BFKL Pomeron exchange, making the contribution of Eq. (28) potentially important for BJKP evolution in the dipole model.

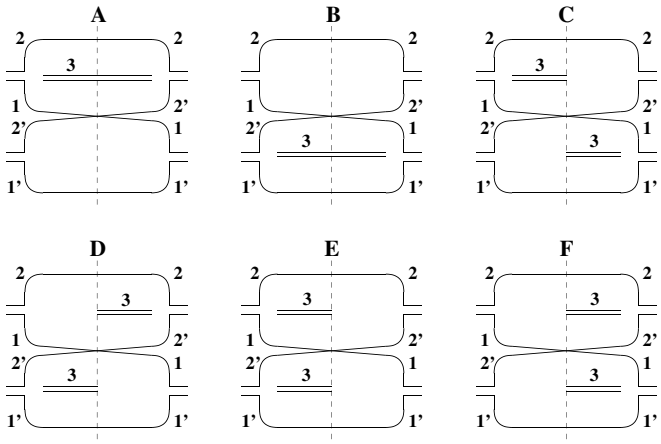

FIG. 8. One step of the quadrupole evolution.

Let us check Eq. (28) for consistency with our earlier results. First, note that if $\underline{x}_2 = \underline{x}_{2'}$ the interactions with line $2/2'$ would cancel and the following equality should be true:

$$
Q(\underline{x}_2, \underline{x}_2, \underline{x}_1, \underline{x}_{1'}, y_1) = S(\underline{x}_1, \underline{x}_{1'}, y_1) = 1 - N(\underline{x}_1, \underline{x}_{1'}, y_1). \qquad (29)
$$

From Eqs. (10) and (15) we can see that Eq. (29) is certainly true for the initial conditions for Eq. (28) given by Q_0 from Eq. (14). Now, as one can explicitly check, putting $\underline{x}_2 = \underline{x}_{2'}$ in Eq. (28) (with $x_{22'} \to \rho$ in the exponent) and assuming that Eq. (29) is true, one readily recovers Eq. (18). Thus, Eq. (28) consistently maps onto Eq. (18) in the limit of Eq. (29).

Using Eq. (29) in Eq. (27) and remembering that due to Eq. (21) the S matrix of a gluon dipole S_G can be expressed in terms of the S matrix of the quark dipole as

$$
S_G(\underline{x}_0, \underline{x}_1, y) = S^2(\underline{x}_0, \underline{x}_1, y), \qquad (30)
$$

we observe that

$$
d(\underline{x}_0, \underline{x}_0, \underline{x}_1, \underline{k}, y) = s(\underline{x}_0, \underline{x}_1, \underline{k}, y), \qquad (31)
$$

which verifies that Eq. (27) is consistent with Eq. (20).

Equation (28), when solved to find Q, can be used to construct d in Eq. (27), which can then be used as the initial condition to the evolution Eq. (26). The quantity

$M(\underline{x}_2, \underline{x}_{2'}, \underline{x}_{\tilde{0}}, Y; \underline{k}_1, y_1)$ obtained this way can be used in Eq. (13) instead of M_0 along with S from Eq. (17) to obtain the evolved contribution of case B considered above to the two-gluon production cross section. Together with the contribution of case A from Eq. (25), it gives us the following expression for the double gluon production cross section in a quark dipole-nucleus scattering [with $\underline{B} = (\underline{x}_0 + \underline{x}_{\tilde{0}})/2$]:

$$\begin{aligned}
\frac{d\sigma^{q\bar{q}A\to q\bar{q}G_1G_2X}}{d^2k_1dy_1d^2k_2dy_2}(\underline{x}_{0\tilde{0}})\Big|_{y_2\gg y_1} = \int d^2B\Big\{ & n_2(\underline{x}_0, \underline{x}_{\tilde{0}}, Y; \underline{x}_1, \underline{x}_{\tilde{1}}, y_1, \underline{x}_2, \underline{x}_{\tilde{2}}, y_2) d^2x_1 d^2x_{\tilde{1}} d^2x_2 d^2x_{\tilde{2}} s(\underline{x}_1, \underline{x}_{\tilde{1}}, \underline{k}_1, y_1) s(\underline{x}_2, \underline{x}_{\tilde{2}}, \underline{k}_2, y_2) \\
& + n_1(\underline{x}_0, \underline{x}_{\tilde{0}}, Y; \underline{x}_1, \underline{x}_{\tilde{1}}, y_2) d^2x_1 d^2x_{\tilde{1}} \frac{\overline{\alpha}_s}{(2\pi)^3} \int d^2x_2 d^2x_{2'} e^{-i\underline{k}_2\cdot\underline{x}_{22'}} \Bigg[\left(\frac{\underline{x}_{21}}{x_{21}^2} - \frac{\underline{x}_{2\tilde{1}}}{x_{2\tilde{1}}^2}\right)\left(\frac{\underline{x}_{2'1}}{x_{2'1}^2} - \frac{\underline{x}_{2'\tilde{1}}}{x_{2'\tilde{1}}^2}\right) \\
& \times M(\underline{x}_2, \underline{x}_{2'}, \underline{x}_{\tilde{1}}, y_2; \underline{k}_1, y_1) S(\underline{x}_2, \underline{x}_{2'}, y_2) - \left(\frac{\underline{x}_{21}}{x_{21}^2} - \frac{\underline{x}_{2\tilde{1}}}{x_{2\tilde{1}}^2}\right)\frac{\underline{x}_{2'1}}{x_{2'1}^2} M(\underline{x}_2, \underline{x}_1, \underline{x}_{\tilde{1}}, y_2; \underline{k}_1, y_1) S(\underline{x}_2, \underline{x}_1, y_2) \\
& - \left(\frac{\underline{x}_{2'1}}{x_{2'1}^2} - \frac{\underline{x}_{2'\tilde{1}}}{x_{2'\tilde{1}}^2}\right)\frac{\underline{x}_{21}}{x_{21}^2} M(\underline{x}_1, \underline{x}_{2'}, \underline{x}_{\tilde{1}}, y_2; \underline{k}_1, y_1) S(\underline{x}_1, \underline{x}_{2'}, y_2) + \frac{\underline{x}_{21}}{x_{21}^2}\frac{\underline{x}_{2'1}}{x_{2'1}^2} M(\underline{x}_1, \underline{x}_1, \underline{x}_{\tilde{1}}, y_2; \underline{k}_1, y_1) \\
& + (1 \leftrightarrow \tilde{1}) \Bigg] \Big\}. \qquad (32)
\end{aligned}$$

Equation (32) is the central result of this section. Together with Eqs. (1), (18), (22), (24), and (26)–(28), it gives us the expression for the two-gluon inclusive cross section for DIS on a nucleus with the effects of nonlinear evolution (18) included.

The structure of Eq. (32) is illustrated in Fig. 9, where, if one pictures the evolution of Eq. (18) as resumming fan diagrams, the diagrams correspond to the first (case A) and the second (cases B and C) terms in Eq. (32). The first term in Eq. (32) corresponds to splitting of the original linear evolution in two, which is described by Eq. (24) for n_2. Then each of the two ladders independently produces a gluon with all the possible splittings happening afterwards. This is illustrated in Fig. 9(a). The second term in Eq. (32) corresponds to nonlinear evolution successively producing both gluons, after which all possible splittings are allowed, as shown in Figs. 9(b) and 9(c), where we have divided the nonlinear evolution into the linear [Fig. 9(b)] and nonlinear [Fig. 9(c)] parts. The linear evolution in this second term in Eq. (32) is given by n_1 from Eq. (22) and by M from the linear part of Eq. (26). This linear evolution leads to production of both gluons #2 and #1 and is illustrated in Fig. 9(b). The initial conditions for Eq. (26) are nonlinear, given by Eqs. (27) and (28). They include ladder splittings and are pictured by the fan diagram in the lower part of Fig. 9(b). One should note, however, that Eq. (26), while being linear in M, has extra factors of $1 - N$ on its right-hand side. That means that evolution of M includes ladder splittings between gluons #2 and #1, one of which is shown in Fig. 9(c). There the evolution leading to creation of gluon #2 is still linear since it is still given by n_1 in the second term on the right-hand side of Eq. (32). However, since the evolution in the rapidity interval between the emitted gluons (evolution of M) is nonlinear, splittings are allowed between gluons #2 and #1, as depicted in Fig. 9(c).

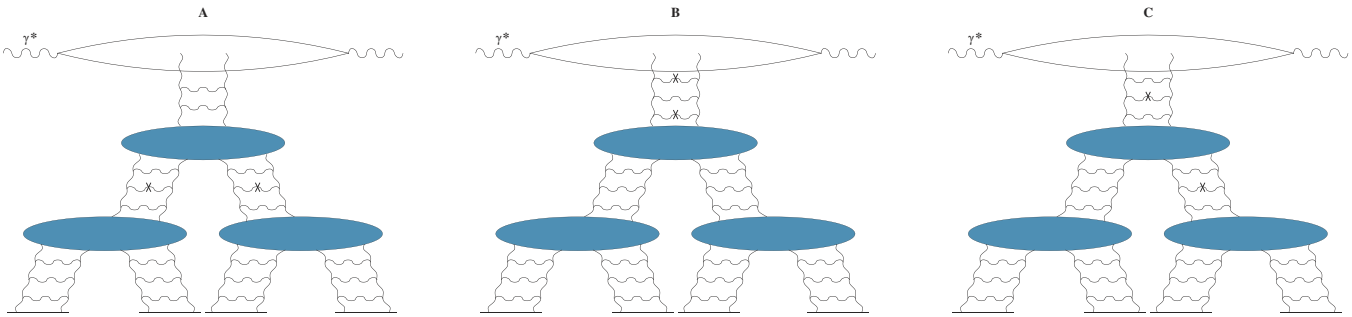

FIG. 9 (color online). Feynman diagrams corresponding to double gluon production cross section given by Eq. (32). The emitted gluons are denoted by crosses.

Diagrams A and B in Fig. 9 are the same as would have been expected from AGK cutting rules [43] (see also [23,54] for similar correspondence between the dipole model results and AGK rules expectations). However, diagram C in Fig. 9, while being included in Eq. (32), is prohibited by AGK cutting rules. Therefore, we seem to observe a direct violation of the AGK rules in QCD. Since AGK rules have never been proven for QCD, one should not be too surprised that they do not work here. It is interesting to note that AGK violation sets in at the level of the two-gluon production: single gluon inclusive production cross section calculated in Ref. [23] adheres to AGK rules and so does the diffractive DIS cross section calculated in Ref. [54].

The violation of AGK cutting rules in Eq. (32) is due to nonlinear terms in Eq. (26), which are in turn due to late-time (after the interaction) gluon emissions at light cone times $\tau > 0$. These terms were not important for the calculation of the total cross section in the dipole model [49]: there they were found to cancel [50]. Thus, if one would try to construct an analogy between the fan diagrams [4] and dipole calculations [9] based on the correspondence of total cross sections, one would omit such terms. Since the fan diagrams seem to adhere to AGK rules, this omission would lead to the erroneous conclusion that AGK rules should work for the production cross section. However, as we have seen above, these late-time emissions are important for single [23] and double inclusive gluon production, violating the AGK rules for the latter. What appears to fail here is the one-to-one correspondence between the fan diagrams and dipole calculations.

Another difference between our result (32) and the direct application of AGK rules to calculating inclusive cross section done in Ref. [24] is that nonlinear splittings may start exactly at the point in rapidity when the softer of the produced gluons is emitted in diagram B or exactly at the point of emission of both gluons #1 and #2 in diagram A. A similar discrepancy was already observed when comparing the single gluon inclusive cross section calculated in Ref. [23] to the results in Ref. [24].

In comparing our result with the formula obtained in Ref. [24] [see Eqs. (30) and (36) there], we note that in a general case we could not cast Eq. (32) in the k_T-factorized form of Ref. [24]. Again, this distinguishes the case of two-gluon production considered here from the case of single gluon production from Ref. [23].

Indeed, our result, given by Eq. (32), is rather complicated, especially keeping in mind that one has to first solve evolution Eqs. (18), (22), (24), (26), and (28) in order to obtain the desired two-particle production cross section. In order to make Eq. (32) easier to implement, it is highly desirable to find some way of simplifying it. Unfortunately, we could not find any simplification of Eq. (32) in the general case. Nevertheless, in certain kinematic regimes Eq. (32) may be simplified. For instance, if the center of mass energy of the collision is not too high or if the transverse momenta of the produced gluons are sufficiently large ($|\underline{k}_1|, |\underline{k}_2| \gtrsim Q_s$), the nonlinear saturation effects, such as ladder splittings, could be neglected. This implies that the diagrams in Figs. 9(a) and 9(c) are small with the linear part of diagram B dominating the cross section. This is the well-known leading-twist result [37], which we will derive from our Eq. (32) in Sec. III C below.

In the opposite kinematic regime of very large center of mass energy of the collision and not too high gluon transverse momenta, saturation effects become important. There one can note that in Figs. 9(b) and 9(c) the evolution between the projectile and the (harder) gluon #2 is linear and is given by a single BFKL ladder exchange. On the other hand, one can show [24] that the diagram in Fig. 9(a) is dominated by the contribution where the triple Pomeron vertex in the evolution between the projectile and gluon #2 is all the way up at the projectile's rapidity. Therefore, the evolution between the projectile and gluon #2 in Fig. 9(a) is given by a double Pomeron exchange and is thus energetically more favorable than the single Pomeron exchange of Figs. 9(b) and 9(c). Since the rest of the three diagrams are parametrically the same, one concludes that Fig. 9(a) dominates in this regime, as was originally shown in Ref. [24]. Keeping only the corresponding first term on the right-hand side of Eq. (32) would significantly simplify the calculation of the cross section: since an analytical solution of Eq. (24) for n_2 exists [49], one would need only to find a solution of Eq. (18), for which there are a number of analytical and numerical results in the literature. However, one has to be careful in neglecting the diagrams in Figs. 9(b) and 9(c). If one is interested in azimuthal two-particle correlations of the produced gluons, then the contributions of graphs in Figs. 9(b) and 9(c) might be more important than the contribution of Fig. 9(a) even deep inside the saturation region [39] .

C. Recovering the leading-twist result

Let us show that Eq. (32) reduces to the usual "leading-twist" k_T-factorization result [37] in the limit of large transverse momenta of the produced gluons. Large transverse momenta correspond to small transverse distances. For short transverse distances, all the evolution equations written above should be linearized since all the nonlinearities would be negligibly small. Therefore, we can right away neglect the first term on the right-hand side of Eq. (32), which contains a splitting (which is a nonlinearity) in the evolution between the target and emitted gluons as shown in Fig. 9(a). In the remaining second term on the right of Eq. (32), we can put all $S \approx 1$ to obtain the linearized expression

$$\frac{d\sigma^{q\bar{q}A\to q\bar{q}G_1G_2X}}{d^2k_1dy_1d^2k_2dy_2}(\underline{x}_{0\tilde{0}})|_{LO} \approx \int d^2B n_1(\underline{x}_0, \underline{x}_{\tilde{0}}, Y; \underline{x}_1, \underline{x}_{\tilde{1}}, y_2) d^2x_1 d^2x_{\tilde{1}} \frac{\overline{\alpha}_s}{(2\pi)^3} \int d^2x_2 d^2x_{2'} e^{-i\underline{k}_2\cdot\underline{x}_{22'}} \Bigg[\left(\frac{\underline{x}_{21}}{x_{21}^2} - \frac{\underline{x}_{2\tilde{1}}}{x_{2\tilde{1}}^2}\right)\left(\frac{\underline{x}_{2'1}}{x_{2'1}^2} - \frac{\underline{x}_{2'\tilde{1}}}{x_{2'\tilde{1}}^2}\right)$$
$$\times M(\underline{x}_2, \underline{x}_{2'}, \underline{x}_{\tilde{1}}, y_2; \underline{k}_1, y_1)|_{\rm lin} - \left(\frac{\underline{x}_{21}}{x_{21}^2} - \frac{\underline{x}_{2\tilde{1}}}{x_{2\tilde{1}}^2}\right)\frac{\underline{x}_{2'1}}{x_{2'1}^2} M(\underline{x}_2, \underline{x}_1, \underline{x}_{\tilde{1}}, y_2; \underline{k}_1, y_1)|_{\rm lin}$$
$$- \left(\frac{\underline{x}_{2'1}}{x_{2'1}^2} - \frac{\underline{x}_{2'\tilde{1}}}{x_{2'\tilde{1}}^2}\right)\frac{\underline{x}_{21}}{x_{21}^2} M(\underline{x}_1, \underline{x}_{2'}, \underline{x}_{\tilde{1}}, y_2; \underline{k}_1, y_1)|_{\rm lin} + \frac{\underline{x}_{21}}{x_{21}^2}\frac{\underline{x}_{2'1}}{x_{2'1}^2} M(\underline{x}_1, \underline{x}_1, \underline{x}_{\tilde{1}}, y_2; \underline{k}_1, y_1)|_{\rm lin}$$
$$+ (1 \leftrightarrow \tilde{1}) \Bigg]. \tag{33}$$

To linearize the evolution equation for M [Eq. (26)], we start by linearizing its initial condition given by d. It is determined by Eq. (27) with Q given by Eq. (28). Therefore, we start with the initial conditions for Eq. (28) given by Eq. (14). Expanding Eq. (14) to the lowest order in the transverse separations (or, equivalently, in Q_{s0}), we obtain

$$Q_0(\underline{x}_2, \underline{x}_{2'}, \underline{x}_1, \underline{x}_{1'})|_{LO} \approx 1 - n_0(\underline{x}_{21}) - n_0(\underline{x}_{2'1'}) - n_0(\underline{x}_{22'}) - n_0(\underline{x}_{11'}) + n_0(\underline{x}_{21'}) + n_0(\underline{x}_{2'1}), \tag{34}$$

where the two-gluon exchange amplitude n_0 is given by the first term in the expansion of N_0 from Eq. (10),

$$n_0(\underline{x}_{21}) = \frac{1}{4} x_{21}^2 Q_{s0}^2 \ln\frac{1}{x_{21}\Lambda}. \tag{35}$$

Let us assume that Eq. (28) independently includes linear BFKL evolution in each of the n_0's in Eq. (34), such that the fully evolved linearized quadrupole amplitude Q is given by

$$q(\underline{x}_2, \underline{x}_{2'}, \underline{x}_1, \underline{x}_{1'}, Y) \equiv Q(\underline{x}_2, \underline{x}_{2'}, \underline{x}_1, \underline{x}_{1'}, Y)|_{\rm lin} = 1 - n(\underline{x}_2, \underline{x}_1, Y) - n(\underline{x}_{2'}, \underline{x}_{1'}, Y) - n(\underline{x}_2, \underline{x}_{2'}, Y) - n(\underline{x}_1, \underline{x}_{1'}, Y) + n(\underline{x}_2, \underline{x}_{1'}, Y) + n(\underline{x}_{2'}, \underline{x}_1, Y), \tag{36}$$

with n determined by the linearized version of Eq. (18) corresponding to BFKL evolution [30]

$$n(\underline{x}_0, \underline{x}_{\tilde{0}}, Y) = n_0(\underline{x}_{0\tilde{0}}) e^{-2\overline{\alpha}_s \ln(x_{0\tilde{0}}/\rho)Y} + \frac{\overline{\alpha}_s}{2\pi}\int_0^Y dy e^{-2\overline{\alpha}_s \ln(x_{0\tilde{0}}/\rho)(Y-y)} \times \int_\rho d^2x_2 \frac{x_{0\tilde{0}}^2}{x_{20}^2 x_{2\tilde{0}}^2}[n(\underline{x}_0, \underline{x}_2, y) + n(\underline{x}_2, \underline{x}_{\tilde{0}}, y)]. \tag{37}$$

After lengthy algebra, one can show that $q(\underline{x}_2, \underline{x}_{2'}, \underline{x}_1, \underline{x}_{1'}, Y)$ from Eq. (36) satisfies the linearized version of Eq. (28)

$$q(\underline{x}_2, \underline{x}_{2'}, \underline{x}_1, \underline{x}_{1'}, y_1) = e^{-\overline{\alpha}_s \ln(x_{21}x_{2'1'}x_{22'}x_{11'}/\rho^4)y_1} Q_0(\underline{x}_2, \underline{x}_{2'}, \underline{x}_1, \underline{x}_{1'})|_{LO} + \frac{\overline{\alpha}_s}{2\pi}\int_0^{y_1} dy e^{-\overline{\alpha}_s \ln(x_{21}x_{2'1'}x_{22'}x_{11'}/\rho^4)(y_1-y)}$$
$$\times \int d^2x_3 \Bigg\{ \left(\frac{\underline{x}_{32}}{x_{32}^2} - \frac{\underline{x}_{31}}{x_{31}^2}\right)\left(\frac{\underline{x}_{32}}{x_{32}^2} - \frac{\underline{x}_{32'}}{x_{32'}^2}\right) q(\underline{x}_3, \underline{x}_{2'}, \underline{x}_1, \underline{x}_{1'}, y) + \left(\frac{\underline{x}_{32'}}{x_{32'}^2} - \frac{\underline{x}_{31'}}{x_{31'}^2}\right)\left(\frac{\underline{x}_{31}}{x_{31}^2} - \frac{\underline{x}_{31'}}{x_{31'}^2}\right)$$
$$\times q(\underline{x}_2, \underline{x}_{2'}, \underline{x}_1, \underline{x}_3, y) - \left(\frac{\underline{x}_{32}}{x_{32}^2} - \frac{\underline{x}_{31}}{x_{31}^2}\right)\left(\frac{\underline{x}_{31}}{x_{31}^2} - \frac{\underline{x}_{31'}}{x_{31'}^2}\right) q(\underline{x}_2, \underline{x}_{2'}, \underline{x}_3, \underline{x}_{1'}, y) - \left(\frac{\underline{x}_{32}}{x_{32}^2} - \frac{\underline{x}_{32'}}{x_{32'}^2}\right)$$
$$\times \left(\frac{\underline{x}_{32'}}{x_{32'}^2} - \frac{\underline{x}_{31'}}{x_{31'}^2}\right) q(\underline{x}_2, \underline{x}_3, \underline{x}_1, \underline{x}_{1'}, y) + \left(\frac{\underline{x}_{32}}{x_{32}^2} - \frac{\underline{x}_{31}}{x_{31}^2}\right)\left(\frac{\underline{x}_{32'}}{x_{32'}^2} - \frac{\underline{x}_{31'}}{x_{31'}^2}\right)[1 - n(\underline{x}_2, \underline{x}_{2'}, y)$$
$$- n(\underline{x}_1, \underline{x}_{1'}, y)] + \left(\frac{\underline{x}_{32}}{x_{32}^2} - \frac{\underline{x}_{32'}}{x_{32'}^2}\right)\left(\frac{\underline{x}_{31}}{x_{31}^2} - \frac{\underline{x}_{31'}}{x_{31'}^2}\right)[1 - n(\underline{x}_2, \underline{x}_1, y) - n(\underline{x}_{2'}, \underline{x}_{1'}, y)] \Bigg\}. \tag{38}$$

This proves that the ansatz of Eq. (36) is indeed the correct linearized quadrupole amplitude Q. Therefore, to construct the initial conditions for the linearized version of Eq. (26), we should substitute $q(\underline{x}_2, \underline{x}_{2'}, \underline{x}_1, \underline{x}_{1'}, Y)$ from Eq. (36) into the linearized version of Eq. (27), obtaining

$$d_{\rm lin}(\underline{x}_2, \underline{x}_{2'}, \underline{x}_{\tilde{0}}, \underline{k}_1, y_1) = \frac{2\overline{\alpha}_s}{(2\pi)^3} \int d^2x_1 d^2x_{1'} e^{-i\underline{k}_1\cdot\underline{x}_{11'}} \left\{ \frac{\underline{x}_{12}}{x_{12}^2} \frac{\underline{x}_{1'2'}}{x_{1'2'}^2} [n(\underline{x}_{2'}, \underline{x}_1, y_1) + n(\underline{x}_2, \underline{x}_{1'}, y_1) - n(\underline{x}_2, \underline{x}_{2'}, y_1) - n(\underline{x}_1, \underline{x}_{1'}, y_1)] \right.$$
$$+ \frac{\underline{x}_{1\tilde{0}}}{x_{1\tilde{0}}^2} \frac{\underline{x}_{1'\tilde{0}}}{x_{1'\tilde{0}}^2} [n(\underline{x}_1, \underline{x}_{\tilde{0}}, y_1) + n(\underline{x}_{1'}, \underline{x}_{\tilde{0}}, y_1) - n(\underline{x}_1, \underline{x}_{1'}, y_1)] - \frac{\underline{x}_{12}}{x_{12}^2} \frac{\underline{x}_{1'\tilde{0}}}{x_{1'\tilde{0}}^2} [n(\underline{x}_2, \underline{x}_{1'}, y_1) + n(\underline{x}_1, \underline{x}_{\tilde{0}}, y_1)$$
$$- n(\underline{x}_2, \underline{x}_{\tilde{0}}, y_1) - n(\underline{x}_1, \underline{x}_{1'}, y_1)] - \frac{\underline{x}_{1\tilde{0}}}{x_{1\tilde{0}}^2} \frac{\underline{x}_{1'2'}}{x_{1'2'}^2} [n(\underline{x}_1, \underline{x}_{2'}, y_1) + n(\underline{x}_{1'}, \underline{x}_{\tilde{0}}, y_1) - n(\underline{x}_{2'}, \underline{x}_{\tilde{0}}, y_1)$$
$$\left. - n(\underline{x}_1, \underline{x}_{1'}, y_1)] \right\}. \tag{39}$$

Here we consider scattering on a large nucleus. The amplitude $n(\underline{x}_1, \underline{x}_{1'}, y)$ depends on the transverse size of the quark-antiquark pair $x_{11'}$ as well as on the transverse position of the dipole. However, the transverse position of the dipole is given by the overall impact parameter $\underline{B}$ in the scattering process. The integrals over $\underline{x}_1$ and $\underline{x}_{1'}$ in Eq. (39), while formally going out to infinity in the transverse direction, are indeed effectively limited to the typical hadronic size on which the concept of a gluon still makes sense. The dependence of n on $\underline{B}$ is smooth for a large nucleus, slowly varying on transverse distances of the order of the typical hadronic size. Therefore, we write (see [23] for a similar approximation)

$$n(\underline{x}_1, \underline{x}_2, y) \approx n(\underline{x}_{12}, \underline{B}, y). \tag{40}$$

With the help of Eq. (40), we rewrite Eq. (39) as

$$d_{\rm lin}(\underline{x}_2, \underline{x}_{2'}, \underline{x}_{\tilde{0}}, \underline{k}_1, y_1) = \frac{\overline{\alpha}_s}{2\pi^2} \frac{1}{\underline{k}_1^2} \int d^2z n(\underline{z}, \underline{B}, y_1) \nabla_z^2 \left(e^{-i\underline{k}_1\cdot\underline{z}} \ln \frac{|\underline{z} - \underline{x}_{2\tilde{0}}||\underline{z} + \underline{x}_{2'\tilde{0}}|}{|\underline{z} - \underline{x}_{22'}||\underline{z}|} \right), \tag{41}$$

where ∇_z^2 is the transverse coordinate gradient squared. Equation (41) is the initial condition for the linearized version of Eq. (26). The latter can be obtained from Eq. (26) by putting all $N = 0$ in it, which yields

$$m(\underline{x}_2, \underline{x}_{2'}, \underline{x}_{\tilde{0}}, Y; \underline{k}_1, y_1) = e^{-\overline{\alpha}_s \ln(x_{2\tilde{0}} x_{2'\tilde{0}} x_{22'}/\rho^3)(Y - y_1)} d_{\rm lin}(\underline{x}_2, \underline{x}_{2'}, \underline{x}_{\tilde{0}}, \underline{k}_1, y_1) + \frac{\overline{\alpha}_s}{2\pi} \int d^2x_4 \int_{y_1}^{Y} dy e^{-\overline{\alpha}_s \ln(x_{2\tilde{0}} x_{2'\tilde{0}} x_{22'}/\rho^3)(Y - y)}$$
$$\times \left\{ \left(\frac{\underline{x}_{42}}{x_{42}^2} - \frac{\underline{x}_{4\tilde{0}}}{x_{4\tilde{0}}^2} \right) \left(\frac{\underline{x}_{42'}}{x_{42'}^2} - \frac{\underline{x}_{4\tilde{0}}}{x_{4\tilde{0}}^2} \right) \left[m(\underline{x}_2, \underline{x}_{2'}, \underline{x}_4, y; \underline{k}_1, y_1) + \int d^2x_a d^2x_b n_1(\underline{x}_4, \underline{x}_{\tilde{0}}, y; \underline{x}_a, \underline{x}_b, y_1) \right.$$
$$\left. \times s(\underline{x}_a, \underline{x}_b, \underline{k}_1, y_1) \right] - \left(\frac{\underline{x}_{42}}{x_{42}^2} - \frac{\underline{x}_{4\tilde{0}}}{x_{4\tilde{0}}^2} \right) \left(\frac{\underline{x}_{42'}}{x_{42'}^2} - \frac{\underline{x}_{42}}{x_{42}^2} \right) m(\underline{x}_4, \underline{x}_{2'}, \underline{x}_{\tilde{0}}, y; \underline{k}_1, y_1) - \left(\frac{\underline{x}_{42}}{x_{42}^2} - \frac{\underline{x}_{42'}}{x_{42'}^2} \right)$$
$$\times \left(\frac{\underline{x}_{42'}}{x_{42'}^2} - \frac{\underline{x}_{4\tilde{0}}}{x_{4\tilde{0}}^2} \right) m(\underline{x}_2, \underline{x}_4, \underline{x}_{\tilde{0}}, y; \underline{k}_1, y_1) \right\}, \tag{42}$$

where we have introduced a linearized amplitude M denoted by

$$m(\underline{x}_2, \underline{x}_{2'}, \underline{x}_{\tilde{0}}, Y; \underline{k}_1, y_1) \equiv M(\underline{x}_2, \underline{x}_{2'}, \underline{x}_{\tilde{0}}, Y; \underline{k}_1, y_1)|_{\rm lin}. \tag{43}$$

The form of Eq. (41) provides us with the following ansatz for the solution of Eq. (42):

$$m(\underline{x}_2, \underline{x}_{2'}, \underline{x}_{\tilde{0}}, Y; \underline{k}_1, y_1) = f(\underline{x}_{2\tilde{0}}, Y; \underline{k}_1, y_1) + f(\underline{x}_{2'\tilde{0}}, Y; \underline{k}_1, y_1) - f(\underline{x}_{22'}, Y; \underline{k}_1, y_1) \tag{44}$$

with f some unknown functions. Substituting the ansatz of Eq. (44) into Eq. (42), one can see that it is a solution of Eq. (42) if

$$f(\underline{x}_{21}, Y; \underline{k}_1, y_1) = \frac{1}{2} \int d^2x_a d^2x_b n_1(\underline{x}_2, \underline{x}_1, Y; \underline{x}_a, \underline{x}_b, y_1) \times s(\underline{x}_a, \underline{x}_b, \underline{k}_1, y_1). \tag{45}$$

The final answer for m is

$$m(\underline{x}_2, \underline{x}_{2'}, \underline{x}_{\tilde{0}}, Y; \underline{k}_1, y_1) = \frac{1}{2} \int d^2x_a d^2x_b [n_1(\underline{x}_2, \underline{x}_{\tilde{0}}, Y; \underline{x}_a, \underline{x}_b, y_1) + n_1(\underline{x}_{2'}, \underline{x}_{\tilde{0}}, Y; \underline{x}_a, \underline{x}_b, y_1) - n_1(\underline{x}_2, \underline{x}_{2'}, Y; \underline{x}_a, \underline{x}_b, y_1)] \times s(\underline{x}_a, \underline{x}_b, \underline{k}_1, y_1). \tag{46}$$

Similar to Eq. (40), we rewrite

$$n_1(\underline{x}_2, \underline{x}_{2'}, Y; \underline{x}_a, \underline{x}_b, y_1) \to n_1(\underline{x}_{22'}, \underline{B}, Y; \underline{x}_a, \underline{x}_b, y_1), \tag{47}$$

with the impact parameter $\underline{B}$. Again, we assume that for a large nucleus n_1 is a slowly varying function of $\underline{B}$. Using Eq. (46) as M in Eq. (33) then yields

$$\frac{d\sigma^{q\bar{q}A\to q\bar{q}G_1G_2X}}{d^2k_1dy_1d^2k_2dy_2}(\underline{x}_{0\bar{0}})|_{LO} \approx \int d^2B n_1(\underline{x}_0, \underline{x}_{\bar{0}}, Y; \underline{x}_1, \underline{x}_{\bar{1}}, y_2) d^2x_1 d^2x_{\bar{1}} \frac{\overline{\alpha}_s}{2(2\pi)^2} \frac{1}{\underline{k}_2^2}$$
$$\times \int d^2z e^{-i\underline{k}_2\cdot\underline{z}} \ln\left(\frac{|\underline{z}-\underline{x}_{1\bar{1}}||\underline{z}+\underline{x}_{1\bar{1}}|}{|\underline{z}|^2}\right) d^2x_a d^2x_b \nabla_z^2 n_1(\underline{z}, \underline{B}, y_2; \underline{x}_a, \underline{x}_b, y_1) s(\underline{x}_a, \underline{x}_b, \underline{k}_1, y_1). \tag{48}$$

Similarly, we rewrite Eq. (20) as

$$s(\underline{x}_a, \underline{x}_b, \underline{k}_1, y_1) = \frac{\overline{\alpha}_s}{(2\pi)^2} \frac{1}{\underline{k}_1^2} \int d^2w e^{-i\underline{k}_1\cdot\underline{w}}$$
$$\times \ln\left(\frac{|\underline{w}-\underline{x}_{ab}||\underline{w}+\underline{x}_{ab}|}{|\underline{w}|^2}\right) \nabla_w^2 N_G(\underline{w}, \underline{B}, y_1). \tag{49}$$

In the linear regime

$$N_G(\underline{w}, \underline{B}, y_1) \approx 2n(\underline{w}, \underline{B}, y_1), \tag{50}$$

with n taken from Eq. (37). Therefore, linearized s can be obtained from Eq. (49) using Eq. (50)

$$s_{\rm lin}(\underline{x}_a, \underline{x}_b, \underline{k}_1, y_1) = \frac{\overline{\alpha}_s}{2\pi^2} \frac{1}{\underline{k}_1^2} \int d^2w e^{-i\underline{k}_1\cdot\underline{w}}$$
$$\times \ln\left(\frac{|\underline{w}-\underline{x}_{ab}||\underline{w}+\underline{x}_{ab}|}{|\underline{w}|^2}\right) \nabla_w^2 n(\underline{w}, \underline{B}, y_1). \tag{51}$$

Defining $\underline{b}_{ab} = (\underline{x}_a + \underline{x}_b)/2$, we relabel the variables of n_1 in Eq. (48) as [23,49]

$$n_1(\underline{z}, \underline{B}, y_2; \underline{x}_a, \underline{x}_b, y_1) \to n_1(\underline{z}, \underline{x}_{ab}, \underline{B} - \underline{b}_{ab}, y_2 - y_1). \tag{52}$$

Then the integrals over $\underline{x}_a$ and $\underline{x}_b$ in Eq. (48) can be written as

$$\int d^2x_{ab} d^2b_{ab} \nabla_z^2 n_1(\underline{z}, \underline{x}_{ab}, \underline{B} - \underline{b}_{ab}, y_2 - y_1) s_{\rm lin}(\underline{x}_a, \underline{x}_b, \underline{k}_1, y_1)$$
$$= \int d^2x_{ab} d^2b_{ab} \nabla_z^2 n_1(\underline{z}, \underline{x}_{ab}, \underline{b}_{ab}, y_2 - y_1) s_{\rm lin}(\underline{x}_a, \underline{x}_b, \underline{k}_1, y_1), \tag{53}$$

where we have put the index indicating that we have to use a linearized amplitude s from Eq. (51) and shifted $\underline{b}_{ab}$ by $\underline{B}$. Using the explicit solution of Eq. (22) [49],

$$\int d^2b_{ab} n_1(\underline{z}, \underline{x}_{ab}, \underline{b}_{ab}, y_2 - y_1)$$
$$= \frac{1}{2\pi\underline{x}_{ab}^2} \int \frac{d\lambda}{2\pi i} e^{2\overline{\alpha}_s\chi(\lambda)(y_2-y_1)} \left(\frac{z}{x_{ab}}\right)^\lambda, \tag{54}$$

with the eigenvalue of the BFKL equation [30,49]

$$\chi(\lambda) = \psi(1) - \frac{1}{2}\psi(\lambda) - \frac{1}{2}\psi(1-\lambda), \tag{55}$$

and with the help of Eq. (51) we rewrite Eq. (53) as

$$\frac{1}{2\pi^2}\nabla_z^2 \int d^2w \left[\int d^2b_{ab} \frac{1}{\nabla_w^4} n_1(\underline{z}, \underline{w}, \underline{b}_{ab}, y_2 - y_1)\right]$$
$$\times \hat{L}_{k_1}(\underline{w}) n(\underline{w}, \underline{B}, y_1), \tag{56}$$

where we have defined the operator for Lipatov's effective vertex [24,30]

$$\hat{L}_k(\underline{z}) \equiv \frac{4\pi\overline{\alpha}_s}{\underline{k}^2} \overleftarrow{\nabla}_z^2 e^{-i\underline{k}\cdot\underline{z}} \to \nabla_z^2. \tag{57}$$

Performing the integrations over $\underline{x}_1$ and $\underline{x}_{1'}$ in Eq. (48) in a similar manner, we finally obtain

$$\frac{d\sigma^{q\bar{q}A\to q\bar{q}G_1G_2X}}{d^2k_1dy_1d^2k_2dy_2}(\underline{x}_{0\bar{0}})|_{LO} \approx \frac{1}{(2\pi)^4} \int d^2B d^2z d^2w \left[\int d^2b_2 \frac{1}{\nabla_z^4} n_1(\underline{x}_{0\bar{0}}, \underline{z}, \underline{b}_2, Y - y_2)\right] \hat{L}_{k_2}(\underline{z})$$
$$\times \left[\int d^2b_1 \frac{1}{\nabla_w^4} n_1(\underline{z}, \underline{w}, \underline{b}_1, y_2 - y_1)\right] \hat{L}_{k_1}(\underline{w}) n(\underline{w}, \underline{B}, y_1). \tag{58}$$

Equation (58) has the structure of three BFKL ladders (two factors of n_1 and one factor of n) with two Lipatov vertices, which are responsible for production of gluons, inserted between them. It is equivalent to the k_T-factorization prediction

for two-gluon production from a single BFKL ladder [see Eq. (30) in Ref. [24]]. We have, therefore, proven that at the leading-twist (large k_T) level, our two-gluon inclusive production cross section (32) reduces to the conventional k_T-factorized expression (58).

Two comments are in order here. First of all, it is a little worrisome that in order to recover the conventional leading-twist result of Eq. (58) we had to expand the initial conditions for the evolution of quadrupole amplitude Q given by Eq. (14) to the lowest order, as shown in Eq. (34). Of course, by doing so, we have shown that the leading-twist formula (58) is included in our full expression (32). Nevertheless, taking a solution of an evolution equation at very short transverse distances does not necessarily imply doing the same to initial conditions of evolution. For instance, if we are interested in the dipole amplitude $N(\underline{x}_0, \underline{x}_{\tilde{0}}, Y)$ at small $\underline{x}_{0\tilde{0}}$, we have to solve the linear part of Eq. (18) with the full initial conditions given by Eq. (10) and not with the leading order initial conditions given by Eq. (35). The kernel of Eq. (18) involves integration over all transverse sizes, including large sizes where multiple rescatterings are important and have to be included. Multiple rescatterings become important at lower energies than the small-x evolution and thus have to be included as an initial condition even for a linear (BFKL) evolution equation. (As one can show, multiple rescatterings in the quasiclassical limit become important at rapidity $y_{\rm mult} \sim \ln 1/\alpha_s$, while the BFKL evolution becomes important at $y_{\rm BFKL} \sim 1/\alpha_s$.) Thus, expanding the initial conditions of Eq. (10) would not be justified if one is interested in the small $\underline{x}_{0\tilde{0}}$ of the amplitude $N(\underline{x}_0, \underline{x}_{\tilde{0}}, Y)$. The effects of saturation in the initial conditions on the short distance/large k_T behavior of the amplitudes and gluon production cross sections have been studied before in Refs. [1,2]. It is exactly these effects that bring in suppression of the nuclear modification factor R^{pA} for the gluon production [1–3]. Therefore, taking the large k_1 and k_2 limits of Eq. (32) more carefully may result in an expression different from the k_T-factorization formula of Eq. (58).

The second observation one has to make is that by now the reader can appreciate the tremendous simplifications one needs to make [e.g., Eq. (34), linearization of all evolution equations, etc.] in order to recover the k_T-factorization formula of Eq. (58). This is strikingly different from the case of single inclusive gluon production considered in Ref. [23]. There, the obtained expression for the cross section was cast in a k_T-factorized form without making any linearization assumptions, i.e., without taking the leading-twist (high-k_T) limit. This k_T-factorization result of Ref. [23] was, indeed, unexpected and very puzzling. However, it is also interesting to observe that it does not hold for the double inclusive gluon production cross section (32). This leaves us guessing whether the preservation of k_T factorization in the formula from Ref. [23] for the single gluon inclusive production cross section after multiple rescatterings and small-x evolution had been included [see Eq. (19) above] was just incidental. A similar breakdown of k_T factorization has been observed recently for $q\bar{q}$ production in pA collisions [41].

IV. VALENCE-QUARK-GLUON PRODUCTION IN PROTON-NUCLEUS COLLISIONS

In this section we calculate the cross section for production of a valence-quark and a gluon in high energy proton-nucleus collisions. Both produced quark and gluon are assumed to have similar rapidity and to be in the proton (deuteron) fragmentation region. In this case, one can treat the proton (deuteron) as a dilute system of partons while the target nucleus is treated as a color glass condensate. The produced quark and gluon then fragment into jets which can be measured. Previously, this approach has been used to calculate valence-quark, photon, and dilepton cross sections in proton (deuteron)-nucleus collisions [31,33]. Here, we extend this formalism to production both of a quark and a gluon. Explicitly, we calculate the differential cross section for the following process:

$$q(p)A \to q(q)g(k)X, \tag{59}$$

given by the amplitude

$$\begin{aligned}\mathcal{M}(q,k;p) &\equiv \langle q(q)g(k)_{\rm out}|q(p)_{\rm in}\rangle \\ &= \langle 0_{\rm out}|a_{\rm out}(k)b_{\rm out}(q)b^{\dagger}_{\rm in}(p)|0_{\rm in}\rangle,\end{aligned} \tag{60}$$

which, using the Lehmann-Symanzik-Zimmermann reduction formalism, can be written as (we set the renormalization factors equal to 1 since we are working at the leading order in α_s)

$$\begin{aligned}\mathcal{M} = g\int d^4x d^4y d^4z d^4r d^4\bar{r} e^{i(q\cdot z + k\cdot r - p\cdot y)}\bar{u}(q) \\ \times [i\overrightarrow{\not\partial}_z]S_F(z,x)\gamma^\nu t^c S_F(x,y) \\ \times [i\overleftarrow{\not\partial}_y]u(p)G^{cb}_{\nu\rho}(x,\bar{r})D^{\rho\mu}_{ba}(\bar{r},r)\epsilon_\mu(k),\end{aligned} \tag{61}$$

where S_F and $G_{\nu\rho}$ are the quark and gluon propagators, respectively, in the classical field background, and $D^{\rho\mu}$ is defined such that

$$\int d^4r G^{0cb}_{\nu\rho}(x,r)D^{\rho\mu}_{ba}(r,y) \equiv \delta^c_a\delta^\mu_\nu\delta^4(x-y), \tag{62}$$

where $G^0_{\nu\rho}$ is the free gluon propagator. This amplitude is shown in Fig. 10 where the quark and gluon lines with a thick dot represent the propagators in the background field as illustrated in Fig. 11.

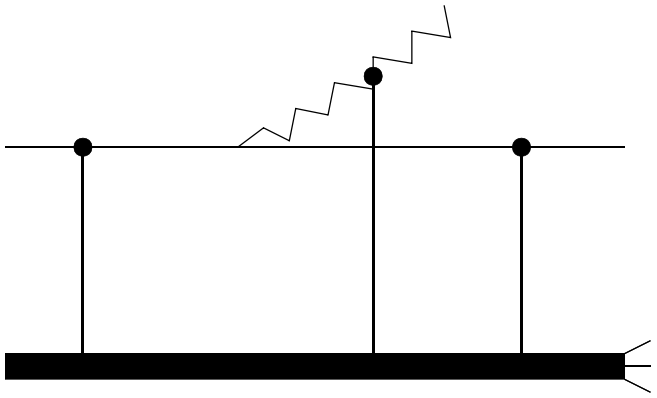

FIG. 10. Production of a quark and a gluon including multiple scattering from the target.

To proceed further, we write the propagators in the above amplitude in momentum space. The amplitude is

$$\mathcal{M} = g \int \frac{d^4k_1}{(2\pi)^4} \frac{d^4k_2}{(2\pi)^4} \frac{d^4k_3}{(2\pi)^4} \bar{u}(q) \not{\epsilon} S_F(q, k_1) \gamma^\nu t^c \times S_F(k_2, p) \not{\epsilon} u(p) G^{cb}_{\nu\rho}(k_2 - k_1, k_3) D^{\rho\mu}_{ba}(k_3, k) \epsilon_\mu(k). \tag{63}$$

The quark and gluon propagators in the classical background field are already known [55,56]. It is useful to separate the free and interacting parts of the propagator in the following. Therefore, we define the interaction part of the propagators in momentum space as (and suppressing the color factor for the moment)

$$\begin{aligned} S_F(q, p) &\equiv (2\pi)^4 \delta^4(p - q) S_F^0(p) + S_F^0(q) \tau_f(q, p) S_F^0(p), \\ G^{\mu\nu}(q, p) &\equiv (2\pi)^4 \delta^4(p - q) G^{0\mu\nu}(p) \\ &\quad + G^{0\mu}_\rho(q) \tau_g(q, p) G^{0\rho\nu}(p), \end{aligned} \tag{64}$$

where the free propagators are

$$\begin{aligned} S_F^0(p) &= i \frac{\not{p}}{p^2} \quad \text{and} \\ G^0_{\mu\nu}(k) &= \frac{i}{k} \left[-g_{\mu\nu} + \frac{\eta_\mu k_\nu + \eta_\nu k_\mu}{\eta \cdot k} \right] \end{aligned} \tag{65}$$

and η_μ is the light cone gauge vector so that $\eta \cdot A \equiv A^- = 0$ defines the gauge in which we are working. In this gauge the interaction part of the gluon propagator in Eq. (64), denoted here by $\tau_g(q, p)$, is diagonal in Lorentz indices, i.e., is proportional to $g_{\mu\nu}$, which allowed us to suppress the Lorentz indices and write it in the form shown in Eq. (64). Such decomposition may not hold in other gauges. Inserting Eqs. (64) into the amplitude and defining

$$\begin{aligned} \mathcal{M}(q, \lambda, k; p) &\equiv M_1 + M_2 + M_3 + M_4 \\ &= \epsilon^{(\lambda)}_\mu(k) [M_1^\mu + M_2^\mu + M_3^\mu + M_4^\mu], \end{aligned} \tag{66}$$

where $\epsilon^{(\lambda)}_\mu(k)$ is the polarization vector of the produced gluon, we get

$$M_1 = -g \bar{u}(q) \not{\epsilon} t^a S_F^0(q + k) \tau_f(q + k, p) u(p), \tag{67}$$

$$M_2 = -g \bar{u}(q) \tau_f(q, p - k) S_F^0(p - k) \not{\epsilon} t^a u(p), \tag{68}$$

$$M_3 = -g \bar{u}(q) \gamma_\nu t^b \tau_g^{ba}(k, p - q) u(p) G_0^{\nu\mu}(p - q) \epsilon_\mu(k), \tag{69}$$

$$M_4 = -g \int d^4l \bar{u}(q) \tau_f(q, p - l) S_F^0(p - l) \times \gamma_\nu t^b \tau_g^{ba}(k, l) u(p) G_0^{\nu\mu}(l) \epsilon_\mu(k), \tag{70}$$

where τ_f and τ_g are given by

$$\tau_f(q, p) \equiv (2\pi) \delta(p^- - q^-) \gamma^- \int d^2x_t e^{i(q_t - p_t) \cdot x_t} [V(x_t) - 1], \tag{71}$$

$$\tau_g(q, p) \equiv 2p^- (2\pi) \delta(p^- - q^-) \int d^2x_t e^{i(q_t - p_t) \cdot x_t} [U(x_t) - 1]. \tag{72}$$

The matrices V and U include all the multiple scatterings of the quark and gluon as they propagate in the strong classical field of the target and are given by

$$V(x_t) \equiv \hat{P} e^{ig \int dz^- A_a^+(x_t, z^-) t_a}, \tag{73}$$

$$U(x_t) \equiv \hat{P} e^{ig \int dz^- A_a^+(x_t, z^-) T_a}. \tag{74}$$

Here t_a and T_a are matrices in the fundamental and adjoint representations of the SU(N) group, respectively, and $A_a^+(x_t, x^-) = -g \delta(x^-) [\rho_a(x_t)/\partial_t^2]$.

With these definitions at hand, extracting an explicit factor of $(2\pi) \delta(p^- - q^- - k^-)$ while using the delta function $\delta(l^- - k^-)$ to do the l^- integration and performing the l^+ integration in M_4 via contour integration using the $(p - l)$ pole, we can write the amplitude as

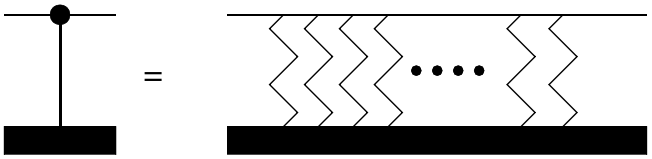

FIG. 11. Multiple scattering of a quark or a gluon on a target.

$$
\begin{aligned}
M_1 &= -ig\frac{1}{2q\cdot k}\bar{u}(q)\not{\epsilon}(\not{q}+\not{k})\gamma^- u(p)t^a[V(q_t+k_t)-(2\pi)^2\delta^2(q_t+k_t)],\\
M_2 &= ig\frac{1}{2p\cdot k}\bar{u}(q)\gamma^-(\not{p}-\not{k})\not{\epsilon}u(p)[V(q_t+k_t)-(2\pi)^2\delta^2(q_t+k_t)]t^a,\\
M_3 &= ig\frac{k^-}{p\cdot q}\bar{u}(q)\gamma_\nu u(p)d^{\nu\mu}(p-q)\epsilon_\mu(k)t^b[U^{ba}(q_t+k_t)-\delta^{ba}(2\pi)^2\delta^2(q_t+k_t)],\\
M_4 &= ig\frac{k^-}{p^-}\int\frac{d^2l_t}{(2\pi)^2}\bar{u}(q)\gamma^-(\not{p}-\not{l})\gamma_\nu u(p)\frac{d^{\nu\mu}(l)}{l_t^2}\epsilon_\mu(k)[V(q_t+l_t)-(2\pi)^2\delta^2(q_t+l_t)]t^b[U^{ba}(k_t-l_t)\\
&\quad-\delta^{ba}(2\pi)^2\delta^2(k_t-l_t)],
\end{aligned}
\tag{75}
$$

where $d^{\mu\nu}(l)$ is related to the free gluon propagator via $d^{\mu\nu}(l)\equiv -il^2G_0^{\mu\nu}(l)$ and $l^-=k^-$, $l^+=-(l_t^2/2q^-)$. We have also set the transverse momentum of the incoming quark to zero without any loss of generality. We show the different diagrams contributing to the amplitude in Fig. 12. They correspond, respectively, to the quark multiply scattering from the target before or after radiating a gluon in Figs. 12(a) and 12(b) and the radiated gluon multiply scattering from the target in Fig. 12(c), while in Fig. 12(d) both the radiated gluon and the final state quark multiply scatter from the target. For the sake of clarity, momenta of the incoming quark and outgoing quark and gluon are shown explicitly in Fig. 12(a).

In Fig. 13 we show one of the diagrams which are suppressed in the high energy limit and do not contribute and, therefore, are not included in Eqs. (75). This is due to the fact that the typical time scale for gluon emission is much longer than the time between rescatterings in the target nucleus. The diagram in Fig. 13 is, therefore, suppressed by a power of center of mass energy and can be safely neglected. Another diagram (not shown), which is suppressed in the high energy limit for the same reason, is when both the initial and final state quark lines as well as the radiated gluon multiply scatter from the target.

To calculate the cross section, we need to square the amplitude $|\mathcal{M}|^2$ (66). There is a factor of $-g_{\mu\nu}+(\frac{1}{\eta\cdot k})\times[k_\mu\eta_\nu+\eta_\mu k_\nu]$ coming from squaring and summing over the polarization of the final state gluon in the light cone gauge which can be used to simplify the expressions. Furthermore, we define $z=q^-/p^-$ so that $1-z=k^-/p^-$. Below, we list the different contributions coming from squaring the amplitude. For reasons which will become clear shortly, we consider the square of M_1+M_2 first. The contribution of the $-g_{\mu\nu}$ term to the squared amplitude is (extracting a factor of g^2 for convenience)

$$
\begin{aligned}
-g_{\mu\nu}(M_1^\mu+M_2^\mu)^\dagger(M_1^\nu+M_2^\nu) &= 16p^-p^-\Big\{\frac{z(1-z)^2}{[zk_t-(1-z)q_t]^2}\mathrm{Tr}[V^\dagger(q_t+k_t)-(2\pi)^2\delta^2(q_t+k_t)]t^at^a[V(q_t+k_t)\\
&\quad-(2\pi)^2\delta^2(q_t+k_t)]+\frac{z(1-z)^2}{k_t^2}\mathrm{Tr}[V(q_t+k_t)-(2\pi)^2\delta^2(q_t+k_t)]t^at^a[V^\dagger(q_t+k_t)\\
&\quad-(2\pi)^2\delta^2(q_t+k_t)]+\Big[(1-z)^2(1+z^2)\frac{q_t^2}{k_t^2[zk_t-(1-z)q_t]^2}+\frac{z^2(1-z^2)}{[zk_t-(1-z)q_t]^2}\\
&\quad-\frac{1-z^2}{k_t^2}\Big]\mathrm{Tr}t^a[V^\dagger(q_t+k_t)-(2\pi)^2\delta^2(q_t+k_t)]t^a[V(q_t+k_t)-(2\pi)^2\delta^2(q_t+k_t)]\Big\},
\end{aligned}
\tag{76}
$$

where Tr denotes trace of color matrices. This term is identical, up to color matrices, to the photon + quark production calculated in Ref. [35]. We now consider contribution of the $[k_\mu\eta_\nu+\eta_\mu k_\nu]$ piece. Using the Dirac equation and the identity $\bar{u}(q)\gamma^-u(p)=2\sqrt{2p^-q^-}$ (valid for on mass shell particles) simplifies the trace algebra considerably and we get

$$
\begin{aligned}
\frac{[k_\mu\eta_\nu+\eta_\mu k_\nu]}{\eta\cdot k}(M_1^\mu+M_2^\mu)^\dagger(M_1^\nu+M_2^\nu) &= 32p^-p^-z^2(1-z)[V^\dagger(q_t+k_t)t^a-t^aV^\dagger(q_t+k_t)]\\
&\quad\times\Big\{\frac{1}{[zk_t-(1-z)q_t]^2}t^aV(q_t+k_t)-\frac{1}{k_t^2}V(q_t+k_t)t^a\Big\}.
\end{aligned}
\tag{77}
$$

Note that this piece has no analog in QED and would vanish in the case of photon emission.

A few remarks regarding the difference between photon and gluon radiation are in order here. In single inclusive photon production in pA collisions as considered in Ref. [35], the photon is emitted by a quark scattering, via multiple gluon exchanges, from a target which is treated as a classical gluon field, generated by recoilless sources of color charge. The photon current is conserved and satisfies $k_\mu M^\mu = 0$ due to gauge invariance. It is, therefore, enough to work in the covariant gauge where the sum over polarization of photons is just $-g_{\mu\nu}$. There is an essential difference between photon and gluon radiation here due to the fact that, in the case of gluon radiation, one also needs to consider radiation of gluons from the target and not just from the quark. This is essential for gauge invariance of the amplitude and current conservation. However, it can be shown that, as long as one works in the light cone gauge, the gluon radiation from the target vanishes identically. This is the case here since we are working in the light cone gauge. However, this means that one needs to keep the full projector $-g_{\mu\nu} + (\frac{1}{\eta\cdot k})[k_\mu \eta_\nu + \eta_\mu k_\nu]$ rather than only the $-g_{\mu\nu}$ piece, which would be the case in the covariant gauge. We now consider the rest of the diagrams:

$$
\begin{aligned}
|M_3^\dagger M_1| &= 16p^- p^- z(1+z^2)\frac{q_t^2 - z q_t\cdot(q_t+k_t)}{q_t^2[zk_t-(1-z)q_t]^2}[U^{\dagger ab}(q_t+k_t)-\delta^{ab}(2\pi)^2\delta^2(q_t+k_t)]\mathrm{Tr} t^b t^a[V(q_t+k_t)\\
&\quad -(2\pi)^2\delta^2(q_t+k_t)],\\
|M_3^\dagger M_2| &= 16p^- p^- z(1+z^2)\frac{q_t\cdot k_t}{q_t^2 k_t^2}[U^{\dagger ab}(q_t+k_t)-\delta^{ab}(2\pi)^2\delta^2(q_t+k_t)]\mathrm{Tr} t^b[V(q_t+k_t)-(2\pi)^2\delta^2(q_t+k_t)]t^a,\\
|M_3|^2 &= 16p^- p^- \frac{z(1+z^2)}{q_t^2}[U^{\dagger ab}(q_t+k_t)-\delta^{ab}(2\pi)^2\delta^2(q_t+k_t)][U^{ca}(q_t+k_t)-\delta^{ca}(2\pi)^2\delta^2(q_t+k_t)]\mathrm{Tr} t^b t^c,\\
|M_3^\dagger M_4| &= -16p^- p^- z(1+z^2)\int\frac{d^2l_t}{(2\pi)^2}\frac{q_t\cdot l_t}{q_t^2 l_t^2}[U^{\dagger ab}(q_t+k_t)-\delta^{ab}(2\pi)^2\delta^2(q_t+k_t)][U^{ca}(k_t-l_t)-\delta^{ca}(2\pi)^2\\
&\quad\times\delta^2(k_t-l_t)]\mathrm{Tr} t^b[V(q_t+l_t)-(2\pi)^2\delta^2(q_t+l_t)]t^c,\\
|M_4^\dagger M_1| &= -16p^- p^- z(1+z^2)\int\frac{d^2l_t}{(2\pi)^2}\frac{(1-z)q_t\cdot l_t - z k_t\cdot l_t}{l_t^2[zk_t-(1-z)q_t]^2}[U^{\dagger ab}(k_t-l_t)-\delta^{ab}(2\pi)^2\delta^2(k_t-l_t)]\mathrm{Tr} t^b[V^\dagger(q_t+l_t)\\
&\quad -(2\pi)^2\delta^2(q_t+l_t)]t^a[V(q_t+k_t)-(2\pi)^2\delta^2(q_t+k_t)],\\
|M_4^\dagger M_2| &= -16p^- p^- (1+z^2)\int\frac{d^2l_t}{(2\pi)^2}\frac{(1-z)l_t^2 + z k_t\cdot l_t}{l_t^2 k_t^2}[U^{\dagger ac}(k_t-l_t)-\delta^{ac}(2\pi)^2\delta^2(k_t-l_t)]\mathrm{Tr} t^c[V^\dagger(q_t+l_t)\\
&\quad -(2\pi)^2\delta^2(q_t+l_t)][V(q_t+k_t)-(2\pi)^2\delta^2(q_t+k_t)]t^a,\\
|M_4|^2 &= 16p^- p^- z(1+z^2)\int\frac{d^2l_t}{(2\pi)^2}\frac{d^2\bar{l}_t}{(2\pi)^2}\frac{l_t\cdot\bar{l}_t}{l_t^2\bar{l}_t^2}[U^{\dagger ac}(k_t-\bar{l}_t)-\delta^{ac}(2\pi)^2\delta^2(k_t-\bar{l}_t)][U^{ab}(k_t-l_t)-\delta^{ab}(2\pi)^2\\
&\quad\times\delta^2(k_t-l_t)]\mathrm{Tr} t^c t^b[V^\dagger(q_t+l_t)-(2\pi)^2\delta^2(q_t+l_t)][V(q_t+\bar{l}_t)-(2\pi)^2\delta^2(q_t+\bar{l}_t)].
\end{aligned}
\tag{78}
$$

Note that, for a given interference term such as $|M_3^\dagger M_1|$, there is also the conjugate term $|M_1^\dagger M_3|$ which is obtained from $|M_3^\dagger M_1|$ by daggering the color matrices. Equations (76)–(78) provide the complete expression for the amplitude squared $|M|^2$. In order to get the invariant cross section, one needs to include the phase space and the flux factors given by $[d^3q/(2\pi)^3](1/2q^-)$, $[d^3k/(2\pi)^3]\times(1/2k^-)$, and $1/2p^-$. Including a factor of $1/2$ coming from averaging over the incoming quark spin and restoring the coupling constant and the overall delta function, the invariant cross section is given by

$$
q^- k^- \frac{d\sigma^{qA\to qgX}}{d^3q d^3k} = \frac{1}{16p^-}\frac{1}{(2\pi)^6}(2\pi)\times\delta(p^- - q^- - k^-)g^2|M|^2. \tag{79}
$$

This is the invariant cross section for production of a quark and gluon in the scattering of a quark on a target nucleus (or a proton at small x) including classical multiple scattering. In order to get the invariant cross section for production of two hadrons or two jets in a proton (deuteron)-nucleus collision, one needs to convolute the cross section given in Eq. (79) with the (valence) quark

distribution function of a proton or deuteron and the quark or gluon fragmentation functions

$$E_{h1}E_{h2}\frac{d\sigma^{pA\to h1h2X}}{d^3q_{h1}d^3k_{h2}} = q_p(x_q)\otimes q^-k^-\frac{d\sigma^{qA\to qgX}}{d^3qd^3k} \otimes D^q_{h1}(z_1)\otimes D^g_{h2}(z_2), \quad (80)$$

where $q_p(x_q)$ is the quark distribution function in a proton and the quark and gluon fragmentation functions are denoted by $D^q_{h1}(z_1)$ and $D^g_{h2}(z_2)$, while $\otimes$ denotes a convolution over Bjorken x for distribution function and over z_1, z_2 for fragmentation functions. The cross section calculated here is valid when one produces two hadrons (or jets) in the forward rapidity region of a proton (deuteron) nucleus collision. It includes the effects of quantum evolution (in x) in the target. To see this, one has to evaluate the Wilson line (U's and V's) correlators in Eqs. (76)–(78) using the Jalilian-Marian-Iancu-McLerran-Weigert-Leonidov-Kovner evolution equation [10]. One can use this cross section in order to investigate two-particle correlations (back-to-back jets) in the RHIC forward rapidity region which can be measured, at RHIC for example, by the Solenoidal Tracker at RHIC detector at rapidity $y = 3.8$.

In order to consider the case when one of the hadrons is produced in the midrapidity region, one needs to allow the possibility that the gluon is radiated not from the valence quark directly, but from anywhere along the (in principle, nonlinear) gluon cascade between the valence quark and the target.

At this point, it is worthwhile to make a connection between the notations used in different sections since they may seem disjoint to a casual reader. The degrees of freedom are indeed the same even though they are denoted differently due to convenience. In Secs. II and III the forward scattering amplitude of a quark-antiquark dipole on the target is denoted by $N(x_t, y_t)$ and can be expressed as

$$N(x_t, y_t) = 1 - \frac{1}{N_c}\mathrm{Tr}\langle V^\dagger(x_t)V(y_t)\rangle, \quad (81)$$

where V is a path-ordered integral in the fundamental representation, used in Sec. IV and defined in Eq. (73). Also, the adjoint dipole amplitude denoted N_G in, for instance, Eq. (21), is equal to

$$N_G(x_t, y_t) = 1 - \frac{1}{N_c^2 - 1}\mathrm{Tr}\langle U^\dagger(x_t)U(y_t)\rangle, \quad (82)$$

where U is the path-ordered integral in the adjoint representation, used in Sec. IV and defined in Eq. (74). Furthermore, the S matrix of the color quadrupole interaction with the target, which is denoted $Q_0(x_t, y_t, z_t, r_t)$ in the classical case and calculated in Eq. (14) and denoted $Q(x_t, y_t, z_t, r_t)$ in the case of quantum evolution included in Eq. (28), can be rewritten in terms of the correlator of four path-ordered exponentials

$$Q(x_t, y_t, z_t, r_t) = \frac{1}{N_c}\mathrm{Tr}\langle V^\dagger(x_t)V(z_t)V^\dagger(r_t)V(y_t)\rangle. \quad (83)$$

The relations in Eqs. (81)–(83) between N, N_G, Q, and the correlators of V's and U's hold even when the quantum evolution is included.

V. CONCLUSIONS

In this paper, we have calculated two cross sections for inclusive two-particle production relevant for the dAu run at RHIC and for the upcoming pA run at LHC. The cross section for two-gluon production at midrapidity for DIS is given by Eq. (32). The expression in Eq. (32) includes all multiple rescatterings of the produced gluons on the target, along with the nonlinear small-x evolution effects [9]. Even though, unlike the single gluon inclusive production cross section of Ref. [23] [see Eq. (19) above], our two-gluon cross section in Eq. (32) cannot be cast in k_T-factorized form, it can be easily generalized to the

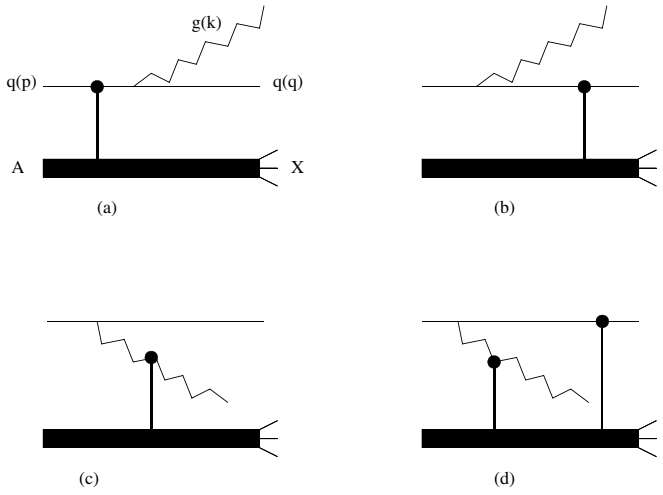

FIG. 12. Diagrams corresponding to M_1, M_2, M_3, M_4.

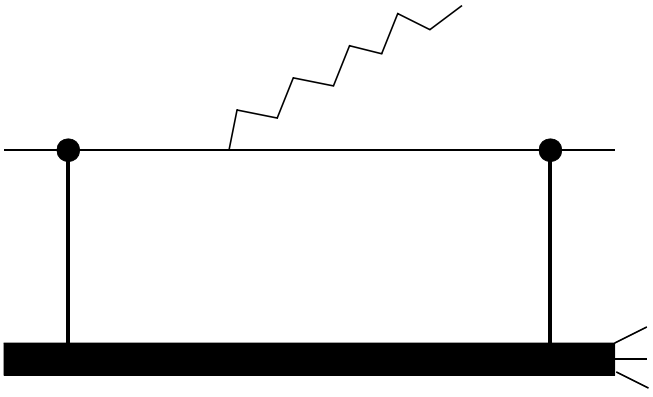

FIG. 13. A typical diagram which is suppressed in the high energy limit and, therefore, not included.

case of proton-nucleus (pA) scattering. Following Ref. [23], we note that the probability $n_1(\underline{x}_{0\tilde{0}}, \underline{x}_{12}, \underline{b}, y)$ of finding a dipole 12 in the original dipole $0\tilde{0}$ can be related to the unintegrated gluon distribution $\phi(\underline{q}, y)$ as

$$\int d^2b \frac{1}{\nabla^2_{x_{12}}} n_1(\underline{x}_{0\tilde{0}}, \underline{x}_{12}, \underline{b}, y) = \frac{(2\pi)^2}{\overline{\alpha}_s} \int d^2q e^{i\underline{q}\cdot\underline{x}_{12}} \phi(\underline{q}, y), \tag{84}$$

where the coefficient on the right-hand side of Eq. (84) has been fixed in order for Eq. (19) to be reducible to the conventional k_T-factorization form of Ref. [37]. The information about the original dipole $0\tilde{0}$ is now contained in its unintegrated gluon distribution $\phi(\underline{q}, y)$. Equation (84) makes generalization of Eq. (19) from DIS to pA rather straightforward: instead of the unintegrated gluon distribution function $\phi(\underline{q}, y)$ of the incoming dipole, one has to use a BFKL evolved unintegrated gluon distribution $\phi(\underline{q}, y)$ of the proton in Eq. (84) and, consequently, in Eq. (19).

To repeat the above procedure for Eq. (32), we have to devise a generalization procedure for the probability of finding two dipoles n_2 as well. To do that, let us first clarify the physical meaning of Eq. (84). The $1/\nabla^2_{x_{12}}$ term in Eq. (84) is due to $\nabla^2_{x_{12}}$, which is usual to the definition of unintegrated gluon distribution in terms of the dipole amplitude [see Eq. (2) in Ref. [2]], and $1/\nabla^4_{x_{12}}$, which is proportional to gluon propagators in a two-gluon exchange amplitude. Thus, in Eq. (84) the gluon distribution is obtained from the dipole probability n_1 by connecting two t-channel exchange gluons to dipole 12 in it. Now, generalization of Eq. (84) to n_2 becomes manifest: one has to connect two exchange gluons to each of the two produced dipoles. The final expression reads

$$\int d^2b_{1\bar{1}} d^2b_{2\bar{2}} \frac{1}{\nabla^2_{x_{1\bar{1}}} \nabla^2_{x_{2\bar{2}}}} n_2(\underline{x}_0, \underline{x}_{\tilde{0}}, Y; \underline{x}_1, \underline{x}_{\bar{1}}, y_1, \underline{x}_2, \underline{x}_{\bar{2}}, y_2) = \frac{(2\pi)^4}{\overline{\alpha}_s^2} \int d^2q d^2l e^{i\underline{q}\cdot\underline{x}_{1\bar{1}} + i\underline{l}\cdot\underline{x}_{2\bar{2}}} \phi_2(\underline{q}, Y - y_1; \underline{l}, Y - y_2), \tag{85}$$

where $b_{1\bar{1}} = (\underline{x}_1 + \underline{x}_{\bar{1}})/2$, $b_{2\bar{2}} = (\underline{x}_2 + \underline{x}_{\bar{2}})/2$, and $\phi_2(\underline{q}, Y - y_1; \underline{l}, Y - y_2)$ is the two-gluon distribution function in the incoming dipole $0\tilde{0}$, with the two gluons having transverse momenta $\underline{q}$ and $\underline{l}$ and rapidities $Y - y_1$ and $Y - y_2$ with respect to the projectile onium.

Analyzing Eq. (32), one can see that for scattering on a large nucleus both n_1 and n_2 come into Eq. (32) integrated over impact parameter(s), as employed in Eqs. (84) and (85). Therefore, using Eqs. (84) and (85) one can rewrite Eq. (32) in terms of single and double unintegrated gluon distributions ϕ and ϕ_2. Taking these distributions for a proton (deuteron) instead of the quarkonium would accomplish generalization of Eq. (32) to the case of $p(d)A$ scattering.

Equations (76)–(78) along with Eq. (79) give us a production cross section for a valence quark and a gluon in the forward rapidity direction in $p(d)A$ scattering. If the correlators of Wilson lines in Eqs. (76)–(78) are averaged in the Gaussian approximation [8], the obtained cross section (79) would reduce to the quasiclassical result containing multiple rescatterings only. (For an explicit evaluation of color averaging of the Wilson lines using a Gaussian weight, see [21,57].) If the Wilson lines are averaged with the weight function obtained from solving the JIMWLK evolution equation [10], then Eq. (79) would include the complete effects of small-x evolution as well.

Before we conclude we would like to make a comment about the applicability of Eqs. (18) and (76)–(78) for RHIC kinematics. Indeed, in deriving these equations, we have assumed for simplicity that the gluons are widely separated in rapidity, $y_2 \gg y_1$. On the other hand, we know that particle production at midrapidity at RHIC appears to be better described by the quasiclassical physics leading to Cronin enhancement. Therefore, if one of the produced particles is at forward rapidity with the other one being at midrapidity, our formulas would apply, though one would not need to include the small-x evolution between the target nucleus and the particle produced at midrapidity, since there the physics is quasiclassical. However, the suppression in R^{dAu}, which is most likely caused by small-x evolution, sets in already at rapidity $\eta = 1$ and continues all the way up to the highest achievable rapidity at RHIC [12,13,15]. That means quantum evolution describes physics at $\eta \geq 1$. Therefore, if both of the produced particles are at rapidity $\eta \geq 1$, say, if $y_1 = 1$ and $y_2 = 3$, we can still have a large rapidity interval between them, $y_2 \gg y_1$, and have quantum evolution between the target and the gluon at y_1 included in Eqs. (18) and (76)–(78). Indeed, the upcoming pA run at the LHC would have a much wider rapidity window, where our results would be even more applicable.

ACKNOWLEDGMENTS

We are grateful to Francois Gelis, Dima Kharzeev, Genya Levin, Al Mueller, and Raju Venugopalan for stimulating and informative discussions. J. J.-M. is supported in part by the U.S. Department of Energy under Grant No. DE-FG02-00ER41132. The work of Yu. K. was supported in part by the U.S. Department of Energy under Grant No. DE-FG02-97ER41014.

APPENDIX

In this appendix we calculate the S matrix of the interaction a quadrupole $2, 2', 1, 1'$ with the target nucleus. The S matrix includes the Glauber-Mueller [7,17,44,48] multiple rescatterings only and is denoted by $Q_0(\underline{x}_2, \underline{x}_{2'}, \underline{x}_1, \underline{x}_{1'})$ in Sec. II above. The possible interac-

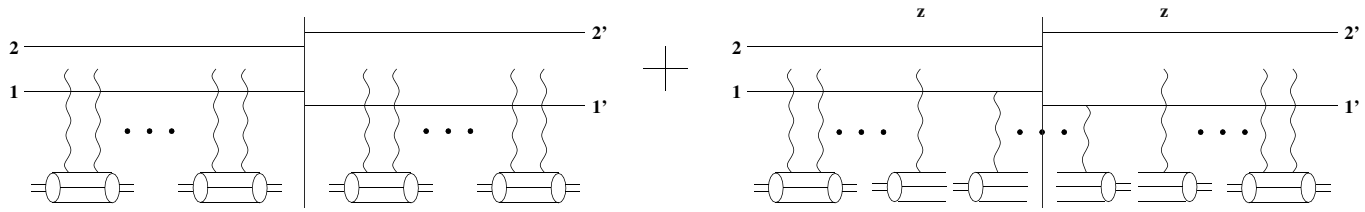

FIG. 14. Leading diagrams contributing to the interaction of a color quadrupole $2, 2', 1, 1'$ with a nuclear target in the large-N_c limit.

tions are shown in Fig. 14. The first term there corresponds to the case where all the interactions in the amplitude and in the complex conjugate amplitude are virtual; i.e., each nucleon exchanges two gluons with the $q\bar{q}$ pair and remains intact. This is the diffractive piece of the interaction [48]. The gluons connect to both the quark and the antiquark lines. This is denoted by leaving the gluon lines disconnected at the top ends. All the virtual exchanges are leading at large N_c. The first diagram in Fig. 14 gives a contribution

$$e^{-x_{21}^2 \ln(1/x_{21}\Lambda) Q_{s0}^2/4} e^{-x_{2'1'}^2 \ln(1/x_{2'1'}\Lambda) Q_{s0}^2/4}, \tag{A1}$$

which is just a product of the S matrices of dipoles 12 and $1'2'$.

The second diagram in Fig. 14 corresponds to the case of at least one *real* interaction: there the nucleon at longitudinal coordinate z interacts with the $q\bar{q}$ pair by a single gluon exchange in the amplitude and in the complex conjugate amplitude. The single gluon exchange breaks up the nucleon in the final state. We will refer to this interaction as real [17,20]. The interaction of the nucleon at z is chosen to be the first real interaction: all prior exchanges are virtual (exchanges to the left of z in the amplitude and to the right of z in the complex conjugate amplitude). After the interaction of nucleon at z, the exchanges can be both real and virtual. However, in the large N_c limit, only those real exchanges contribute where gluons connect to either lines 1 and $1'$ or lines 2 and $2'$. The color structure is similar to the dipole model [49]: the nucleon at z splits the original single quark loop $2, 2', 1, 1'$ into two, and the successive interactions can take place only within each of the two resulting loops.

The contribution of the second graph in Fig. 14 is therefore

$$\begin{aligned}\int_0^L \frac{dz}{L} e^{-1/4[x_{21}^2 \ln(1/x_{21}\Lambda) + x_{2'1'}^2 \ln(1/x_{2'1'}\Lambda)] Q_{s0}^2 z/L} \\ \times \left(-\frac{1}{4} Q_{s0}^2\right) [x_{22'}^2 \ln(1/x_{22'}\Lambda) + x_{11'}^2 \ln(1/x_{11'}\Lambda) \\ + x_{21'}^2 \ln(1/x_{21'}\Lambda) + x_{2'1}^2 \ln(1/x_{2'1}\Lambda)] \\ \times e^{-1/4[x_{22'}^2 \ln(1/x_{22'}\Lambda) + x_{11'}^2 \ln(1/x_{11'}\Lambda)] Q_{s0}^2 (L-z)/L}.\end{aligned} \tag{A2}$$

In Eq. (A2) the first exponent resums all virtual interactions before the first real interaction at z, the second exponent resums all the real and virtual interactions with dipoles $22'$ and $11'$ following the first real interaction, and the term in between accounts for the first real interaction itself. We also average over the longitudinal coordinate z, which varies from 0 to L, where L is the longitudinal extent of the nucleus at a given impact parameter.

Performing the integration over z in Eq. (A2) and adding to it the contribution from Eq. (A1) yields Eq. (14) in the text.

[1] D. Kharzeev, E. Levin, and L. McLerran, Phys. Lett. B **561**, 93 (2003).
[2] D. Kharzeev, Y.V. Kovchegov, and K. Tuchin, Phys. Rev. D **68**, 094013 (2003).
[3] J. L. Albacete, N. Armesto, A. Kovner, C. A. Salgado, and U. A. Wiedemann, Phys. Rev. Lett. **92**, 082001 (2004).
[4] L.V. Gribov, E. M. Levin, and M. G. Ryskin, Phys. Rep. **100**, 1 (1983).
[5] A. H. Mueller and J.W. Qiu, Nucl. Phys. **B268**, 427 (1986).
[6] J. P. Blaizot and A. H. Mueller, Nucl. Phys. **B289**, 847 (1987).
[7] L. D. McLerran and R. Venugopalan, Phys. Rev. D **49**, 2233 (1994); **49**, 3352 (1994); **50**, 2225 (1994).
[8] Y.V. Kovchegov, Phys. Rev. D **54**, 5463 (1996); **55**, 5445 (1997); J. Jalilian-Marian, A. Kovner, L. D. McLerran, and H. Weigert, Phys. Rev. D **55**, 5414 (1997).
[9] I. Balitsky, Nucl. Phys. **B463**, 99 (1996); Y.V. Kovchegov, Phys. Rev. D **60**, 034008 (1999); **61**, 074018 (2000).
[10] J. Jalilian-Marian, A. Kovner, A. Leonidov, and H. Weigert, Nucl. Phys. **B504**, 415 (1997); Phys. Rev. D **59**, 014014 (1999); **59**, 034007 (1999); **59**, 099903(E) (1999); J. Jalilian-Marian, A. Kovner, and H. Weigert, Phys. Rev. D **59**, 014015 (1999); E. Iancu, A. Leonidov, and L. D. McLerran, Phys. Lett. B **510**, 133 (2001); E.

Iancu and L. D. McLerran, Phys. Lett. B **510**, 145 (2001); E. Ferreiro, E. Iancu, A. Leonidov, and L. McLerran, Nucl. Phys. **A703**, 489 (2002);E. Iancu, K. Itakura, and L. D. McLerran, Nucl. Phys. **A708**, 327 (2002); for a review, see E. Iancu and R. Venugopalan, hep-ph/0303204.

[11] M. Gyulassy and L. D. McLerran, nucl-th/0405013.

[12] BRAHMS Collaboration, R. Debbe *et al.*, J. Phys. G **30**, S759 (2004).

[13] BRAHMS Collaboration, I. Arsene *et al.*, nucl-ex/0403005.

[14] PHENIX Collaboration, M. Liu *et al.*, nucl-ex/0403047.

[15] PHOBOS Collaboration, P. Steinberg, Proceedings of the Quark Matter 2004 Conference, Oakland, California, January 2004 (to be published).

[16] STAR Collaboration, L. Barnby *et al.*, J. Phys. G **30**, S1121 (2004).

[17] Y.V. Kovchegov and A. H. Mueller, Nucl. Phys. **B529**, 451 (1998).

[18] B. Z. Kopeliovich, A.V. Tarasov, and A. Schafer, Phys. Rev. C **59**, 1609 (1999).

[19] A. Dumitru and L. D. McLerran, Nucl. Phys. **A700**, 492 (2002).

[20] Y.V. Kovchegov, Phys. Rev. D **64**, 114016 (2001); **68**, 039901(E) (2003).

[21] A. Kovner and U. A. Wiedemann, Phys. Rev. D **64**, 114002 (2001).

[22] M. Braun, Eur. Phys. J. C **16**, 337 (2000).

[23] Y.V. Kovchegov and K. Tuchin, Phys. Rev. D **65**, 074026 (2002).

[24] M. A. Braun, Phys. Lett. B **483**, 105 (2000).

[25] J.W. Cronin, H. J. Frisch, M. J. Shochet, J. P. Boymond, R. Mermod, P. A. Piroue, and R. L. Sumner, Phys. Rev. D **11**, 3105 (1975).

[26] B. Z. Kopeliovich, J. Nemchik, A. Schafer, and A.V. Tarasov, Phys. Rev. Lett. **88**, 232303 (2002).

[27] A. Accardi and M. Gyulassy, Phys. Lett. B **586**, 244 (2004); X. N. Wang, Phys. Rev. C **61**, 064910 (2000); Phys. Lett. B **565**, 116 (2003); G. G. Barnafoldi, G. Papp, P. Levai, and G. Fai, nucl-th/0307062; for a review, see M. Gyulassy, I. Vitev, X. N. Wang, and B.W. Zhang, *Quark Gluon Plasma 3*, edited by R. C. Hwa and X. N. Wang (World Scientific, Singapore, 2003), pp. 123–191; B. Z. Kopeliovich, A.V. Tarasov, and A. Schafer, Phys. Rev. C **59**, 1609 (1999).

[28] R. Baier, A. Kovner, and U. A. Wiedemann, Phys. Rev. D **68**, 054009 (2003).

[29] J. Jalilian-Marian, Y. Nara, and R. Venugopalan, Phys. Lett. B **577**, 54 (2003).

[30] E. A. Kuraev, L. N. Lipatov, and V. S. Fadin, Zh. Eksp. Teor. Fiz. **72**, 377 (1977) [Sov. Phys. JETP **45**, 199 (1977)]; I. I. Balitsky and L. N. Lipatov, Yad. Fiz. **28**, 1597 (1978) [Sov. J. Nucl. Phys. **28**, 822 (1978)].

[31] A. Dumitru and J. Jalilian-Marian, Phys. Rev. Lett. **89**, 022301 (2002); Phys. Lett. B **547**, 15 (2002).

[32] E. Iancu, K. Itakura, and D. N. Triantafyllopoulos, Nucl. Phys. **A742**, 182 (2004).

[33] F. Gelis and J. Jalilian-Marian, Phys. Rev. D **67**, 074019 (2003); **66**, 094014 (2002); **66**, 014021 (2002); J. Jalilian-Marian, Nucl. Phys. **A739**, 319 (2004); R. Baier, A. H. Mueller, and D. Schiff, Nucl. Phys. **A741**, 358 (2004).

[34] B. Z. Kopeliovich, J. Raufeisen, A.V. Tarasov, and M. B. Johnson, Phys. Rev. C **67**, 014903 (2003); M. B. Johnson *et al.*, Phys. Rev. C **65**, 025203 (2002); B. Z. Kopeliovich, J. Raufeisen, and A.V. Tarasov, Phys. Lett. B **503**, 91 (2001); S. J. Brodsky, A. Hebecker, and E. Quack, Phys. Rev. D **55**, 2584 (1997).

[35] J. Jalilian-Marian, nucl-th/0402080.

[36] D. Kharzeev, Y.V. Kovchegov, and K. Tuchin, hep-ph/0405045.

[37] E. M. Levin and M. G. Ryskin, Yad. Fiz. **21**, 1072 (1975).

[38] Y.V. Kovchegov and K. L. Tuchin, Nucl. Phys. **A708**, 413 (2002); **A717**, 249 (2003).

[39] D. Kharzeev, E. Levin, and L. D. McLerran, hep-ph/0403271.

[40] STAR Collaboration, A. Ogawa, Proceedings of DIS2004, Štrbské Pleso, Slovakia, April 2004 (to be published).

[41] K. Tuchin, Phys. Lett. B **593**, 66 (2004); J. P. Blaizot, F. Gelis, and R. Venugopalan, Nucl. Phys. **A743**, 13 (2004).

[42] N. N. Nikolaev, W. Schafer, B. G. Zakharov, and V. R. Zoller, Zh. Eksp. Teor. Fiz. **124**, 491 (2003)[J. Exp. Theor. Phys. **97**, 441 (2003)].

[43] V. A. Abramovsky, V. N. Gribov, and O.V. Kancheli, Yad. Fiz. **18**, 595 (1973)[Sov. J. Nucl. Phys. **18**, 308 (1974)].

[44] A. H. Mueller, Nucl. Phys. **B335**, 115 (1990).

[45] A. Leonidov and D. Ostrovsky, hep-ph/9811417; Eur. Phys. J. C **16**, 683 (2000); Phys. Rev. D **62**, 094009 (2000).

[46] G. P. Lepage and S. J. Brodsky, Phys. Rev. D **22**, 2157 (1980).

[47] N. N. Nikolaev and B. G. Zakharov, Z. Phys. C **49**, 607 (1991).

[48] Y.V. Kovchegov and L. D. McLerran, Phys. Rev. D **60**, 054025 (1999); **62**, 019901(E) (2000).

[49] A. H. Mueller, Nucl. Phys. **B415**, 373 (1994); A. H. Mueller and B. Patel, Nucl. Phys. **B425**, 471 (1994); A. H. Mueller, Nucl. Phys. **B437**, 107 (1995).

[50] Z. Chen and A. H. Mueller, Nucl. Phys. **B451**, 579 (1995).

[51] R. Baier, Y. L. Dokshitzer, A. H. Mueller, and D. Schiff, Nucl. Phys. **B531**, 403 (1998).

[52] J. Bartels, Nucl. Phys. **B151**, 293 (1979); **B175**, 365 (1980); T. Jaroszewicz, Acta Phys. Pol. B **11**, 965 (1980); J. Kwiecinski and M. Praszalowicz, Phys. Lett. **94B**, 413 (1980).

[53] G. P. Korchemsky, J. Kotanski, and A. N. Manashov, Phys. Rev. Lett. **88**, 122002 (2002).

[54] Y.V. Kovchegov and E. Levin, Nucl. Phys. **B577**, 221 (2000).

[55] A. Hebecker and H. Weigert, Phys. Lett. B **432**, 215 (1998).

[56] A. Ayala, J. Jalilian-Marian, L. D. McLerran, and R. Venugopalan, Phys. Rev. D **52**, 2935 (1995)**53**, 458 (1996); E. Iancu, A. Leonidov, and L. D. McLerran, Nucl. Phys. **A692**, 583 (2001).

[57] J. P. Blaizot, F. Gelis, and R. Venugopalan, Nucl. Phys. **A743**, 57 (2004).